Multichannel resonance parametrization of πN scattering amplitudes

D. M. Manley and E. M. Saleski*
Department of Physics and Center for Nuclear Research, Kent State University, Kent, Ohio 44242
(Received 24 June 1991; revised manuscript received 9 March 1992)

A new manifestly time-reversal invariant and unitary parametrization of S-matrix elements is described. The method is simpler than the K-matrix approach in that resonance parameters are parametrized directly. The technique is used to extract resonance parameters from partial-wave amplitudes for $\pi N \to \pi N$ and from isobar-model amplitudes for $\pi N \to \pi\pi N$. Resonance parameters obtained from this approach are tabulated and compared to predictions of quark-model calculations and to results of previous work.

PACS number(s): 14.20.Gk, 11.80.Gw, 13.30.Eg, 13.75.Gx

I. INTRODUCTION

The study of nucleon resonances has been an area of growing interest in recent years; part of this interest stems from the construction of the Continuous Electron Beam Accelerator Facility (CEBAF), which is planned to have a major experimental program for investigating the electromagnetic properties of the nucleon and its excited states. Studies of the hadronic properties of nucleon resonances provide complementary information to that which can be learned using electromagnetic probes; indeed, for an unambiguous understanding of the decay properties of nucleon resonances, information deduced from studies of hadronic reactions such as $\pi N \to \pi N$, $\pi N \to \eta N$, and $\pi N \to \pi\pi N$ is crucial. The present work uses partial-wave amplitudes determined from measurements of πN elastic scattering and single-pion production to provide new information on the hadronic couplings of nucleon resonances with masses below about 2 GeV.

The most recent and extensive study of $\pi N \to \pi\pi N$ reactions within the framework of the isobar model extended over the center-of-mass (c.m.) energy range 1320 to 1930 MeV and included over 30% more events than previous analyses [1]. A primary assumption of the isobar model is that all the reactions are approximately describable by a coherent superposition of quasi-two-body channels. The inelastic channels considered in Ref. [1] include $\pi\Delta$, $\rho_3 N$, $\rho_1 N$, ϵN, and πN^*, where ϵ denotes the strong s-wave isoscalar $\pi\pi$ interaction and N^* denotes the Roper resonance. Starting with the quasi-two-body amplitudes from Ref. [1] and with partial-wave amplitudes from elastic phase-shift analyses, we apply the constraints of unitarity to fit the T-matrix amplitudes and extract resonance parameters (mass, total and partial widths, relative signs of coupling). Two previous multichannel studies [2,3] extracted resonance parameters by first applying unitarity through a K-matrix approach. The first of these by Longacre and Dolbeau at Saclay [2] was based on quasi-two-body amplitudes at c.m. energies between 1360 and 1760 MeV [4]; the second by a Berkeley-Stanford Collaboration [3] was based on quasi-two-body amplitudes at c.m. energies between 1300 and 1990 MeV [5]. Both studies used elastic partial-wave amplitudes from two, now obsolete, phase-shift analyses [6,7]. The present work uses elastic partial-wave amplitudes from the Carnegie Mellon–Berkeley (CMB) solution [8] and the Karlsruhe-Helsinki (KH) solution [9]. The nominal resonance parameters of the Particle Data Group [10] are determined primarily from these 1980 solutions. Since completing the present work, a new elastic phase-shift analysis extending to a c.m. energy of about 2.2 GeV was published by Arndt *et al.* [11].

II. PARAMETRIZATION OF THE AMPLITUDES

For each partial wave, the elastic phase-shift analyses and isobar-model analyses determine elements of the nuclear transition matrix, which is related to the unitary scattering matrix by $S=1+2iT$. In the K-matrix approach, the unitarity of S is ensured by constructing it from a real, symmetric K matrix; i.e., we write

$$S=(1+iK)(1-iK)^{-1} . \tag{1}$$

A drawback of this approach is that some further T-matrix analysis must be performed to extract resonance parameters; furthermore, the resonance parameters (e.g., pole positions) are sensitive to experimental fluctuations in the data and to the assumed dimensionality of the matrix (equal to the number of channels being parametrized) [3]. As stated in Ref. [2], "the K-matrix formalism is a convenient way to parametrize the amplitudes, including unitarity, but does not allow a good determination of the resonance parameters."

In the so-called T-matrix approach [12], the multichannel S matrix is constructed from the sum $S=B+R$, where B is a unitary background matrix and R is a resonance matrix with elements given by the Breit-Wigner form:

$$R_{ij}=2i\frac{\frac{1}{2}\sqrt{\gamma_i\gamma_j}\,e^{i(\theta_i+\theta_j)}}{m-W-\frac{1}{2}i\sum_k \gamma_k} . \tag{2}$$

*Present address: Stanford Linear Accelerator Center, Bin 55, Stanford, CA 94309.

Here W is the c.m. energy, m is the mass of the resonance, and γ_k is the partial width for decay of the resonance into the kth channel. The difficulties with this approach are that unitarity of S is nontrivial to implement and, since only a single resonance is assumed, it can be used to fit amplitudes *only* in the restricted energy region of a pole [2,3].

Our approach was inspired somewhat by the method of Novoseller [12]. First we write the S matrix as a product of background and resonant S matrices:

$$S=S_R^T S_B S_R \ . \tag{3}$$

Here both S_B and S_R are unitary and S_R^T is the transpose of S_R; the matrix S_B is constructed from a real, symmetric background K matrix:

$$S_B=(1+iK_B)(1-iK_B)^{-1} \ . \tag{4}$$

Explicit pole terms in K_B were not included. Note that, at energies away from resonance poles, $S_R\approx 1$ and $S\approx S_B$. In order to limit the number of free parameters, we represented K_B by the form

$$K_B=\alpha\rho^{1/2}O\rho^{1/2} \ , \tag{5}$$

where α was parametrized as a polynomial function in W, $\rho^{1/2}$ is a diagonal phase-space matrix (see later), and O is a real, symmetric orthogonal matrix. The manner in which the O matrix was constructed is best illustrated by explicit examples. For one channel, we have trivially, $O=1$. For two channels, it is simple to show that

$$O=\begin{bmatrix} c_1 & s_1 \\ s_1 & -c_1 \end{bmatrix} , \tag{6}$$

where $c_i=\cos\theta_i$ and $s_i=\sin\theta_i$. For three channels, we have

$$O=\begin{bmatrix} c_2 & s_2 & 0 \\ s_2 & -c_2 & 0 \\ 0 & 0 & 1 \end{bmatrix}\begin{bmatrix} 1 & 0 & 0 \\ 0 & c_1 & s_1 \\ 0 & s_1 & -c_1 \end{bmatrix}\begin{bmatrix} c_2 & s_2 & 0 \\ s_2 & -c_2 & 0 \\ 0 & 0 & 1 \end{bmatrix} , \tag{7}$$

and for four channels, we have

$$O=\begin{bmatrix} c_3 & s_3 & 0 & 0 \\ s_3 & -c_3 & 0 & 0 \\ 0 & 0 & 1 & 0 \\ 0 & 0 & 0 & 1 \end{bmatrix}\begin{bmatrix} 1 & 0 & 0 & 0 \\ 0 & c_2 & s_2 & 0 \\ 0 & s_2 & -c_2 & 0 \\ 0 & 0 & 0 & 1 \end{bmatrix}\begin{bmatrix} 1 & 0 & 0 & 0 \\ 0 & 1 & 0 & 0 \\ 0 & 0 & c_1 & s_1 \\ 0 & 0 & s_1 & -c_1 \end{bmatrix}$$
$$\times\begin{bmatrix} 1 & 0 & 0 & 0 \\ 0 & c_2 & s_2 & 0 \\ 0 & s_2 & -c_2 & 0 \\ 0 & 0 & 0 & 1 \end{bmatrix}\begin{bmatrix} c_3 & s_3 & 0 & 0 \\ s_3 & -c_3 & 0 & 0 \\ 0 & 0 & 1 & 0 \\ 0 & 0 & 0 & 1 \end{bmatrix} . \tag{8}$$

For the general case of n channels ($n>2$), the O matrix is found by first embedding a 2×2 O matrix in the lower right-hand corner of an $n\times n$ identity matrix. This matrix is then left and right multiplied by an $n\times n$ identity matrix with a 2×2 O matrix (of another angle) embedded one position towards the upper left corner. The procedure of left and right multiplying is repeated until a 2×2 O matrix is in the upper left corner. This procedure gives the full $n\times n$ O matrix after $2n-4$ matrix multiplications are performed. The n-channel K_B so defined depends on n independent parameters, namely α and the $n-1$ angles, θ_i ($i=1,\ldots,n-1$), which were parametrized as linear functions of W.

The matrix S_R in Eq. (3) was constructed to have the form

$$S_R=S_1^{1/2}S_2^{1/2}\cdots S_N^{1/2} \ , \tag{9}$$

where N is the number of resonances being parametrized and $S_k^{1/2}$ is a symmetric, unitary matrix that describes the kth resonance of mass m_k and total width Γ_k; we treated Eq. (9) as an energy-dependent expansion in the sense that $m_j>m_k$ if $j>k$. The form of $S_k^{1/2}$ is given by

$$S_k^{1/2}=1+[i-x_k+(1+x_k^2)^{1/2}]T_k \ , \tag{10}$$

where

$$x_k=\frac{m_k-W}{\frac{1}{2}\sum_r \gamma_r^k} \tag{11}$$

and T_k has elements given by the Breit-Wigner form

$$(T_k)_{ij}=\frac{\frac{1}{2}\epsilon_i^k\epsilon_j^k(\gamma_i^k\gamma_j^k)^{1/2}}{m_k-W-\frac{1}{2}i\sum_r \gamma_r^k} \ . \tag{12}$$

Here γ_i^k denotes the energy-dependent partial width for decay of the kth resonance into the ith channel and ϵ_i^k is the relative sign of the coupling. The form of $S_k^{1/2}$ was constructed such that its square gives $S_k=1+2iT_k$; thus, in the vicinity of the kth resonance, $S\approx S_k$ and $T\approx T_k$, if there is no appreciable overlap with nearby resonances and if nonresonant background is negligible (i.e., if $S_B\approx 1$).

The energy dependence of the partial width γ_j^k is given by $\gamma_j^k=\lambda_k\rho_j(W)$, where λ_k is a constant and $\rho_j(W)$ is related to an element of the phase-space matrix in Eq. (5). In general, the elements have the form

$$(\rho^{1/2})_{ij}=\sqrt{\rho_i(W)}\delta_{ij} \ ; \tag{13}$$

for $\rho_j(m_k)>0$, we have

$$\gamma_j^k=\Gamma_j^k\frac{\rho_j(W)}{\rho_j(m_k)} \ , \tag{14}$$

where Γ_j^k is the partial width for decay of the kth resonance into the ith channel, evaluated at $W=m_k$. The total width of the resonance is then

$$\Gamma_k=\sum_r \Gamma_r^k \ . \tag{15}$$

The specific form of $\rho_j(W)$ depends on the decay channel. For decay of a resonance into two "stable" particles (e.g., πN, ηN, ωN, $K\Lambda$), we parametrized $\rho_j(W)$ by the form

$$\rho_j(W)=\frac{q_j}{W}B_{l_j}^2(q_jR) \ , \tag{16}$$

where q_j is the relative momentum of the two particles, l_j is the orbital angular momentum between the pair, $R=1$ fm is an interaction radius, and $B_{l_j}^2$ is a Blatt-Weisskopf barrier-penetration factor [13]. For $x \ll 1$, $B_l^2(x) \sim x^{2l}$ and for $x \gg 1$, $B_l^2(x) \sim 1$; thus, the energy-dependent partial widths have the proper analytic threshold behavior ($\sim q_j^{2l_j+1}$) and become constant at large energies. We determined the optimum value of the interaction radius by fitting amplitudes for the F_{37} and G_{17} partial waves with fixed values of R between 0.25 and 1.25 fm and minimizing the total χ^2. The results of this procedure gave a value consistent with that used in the K-matrix approach of Longacre and Dolbeau [2].

Now consider the quasi-two-body decay of a resonance into a channel consisting of a stable particle and an isobar (e.g., $\pi\Delta$, ρN, ϵN). Here we must integrate over the mass $\mathcal{M}$ of the isobar, which is assumed to decay into stable particles having masses m_1 and m_2,

$$\rho_j(W)=\int_{m_1+m_2}^{W-m_3}\sigma(\mathcal{M})\frac{q_j}{W}B_{l_j}^2(q_jR)d\mathcal{M}\ . \tag{17}$$

Note that q_j is now a function of $\mathcal{M}$. For simplicity, the distribution function $\sigma(\mathcal{M})$ was taken to have the form

$$\sigma(\mathcal{M})=\frac{1}{\pi}\frac{\Gamma_0/2}{(\mathcal{M}-M_0)^2+(\Gamma_0/2)^2}\ , \tag{18}$$

where M_0 and Γ_0 are constants (see Table I). Note that in the limit $\Gamma_0 \to 0$, $\sigma(\mathcal{M}) \to \delta(\mathcal{M}-M_0)$. For the quasi-two-body decay of a resonance into a channel consisting of two isobars (e.g., $\rho\Delta$), we must integrate over the mass of each isobar

$$\rho_j(W)=\int\int\sigma(\mathcal{M}_1)\sigma(\mathcal{M}_2)\frac{q_j}{W}B_{l_j}^2(q_jR)d\mathcal{M}_1d\mathcal{M}_2\ . \tag{19}$$

Here q_j is a function of $\mathcal{M}_1$ and $\mathcal{M}_2$.

Throughout this paper, the symbol ϵ is used only as a convenient notation for the s-wave isoscalar $\pi\pi$ interaction below about 1 GeV in the $\pi\pi$ invariant mass. The notation and parameters for the ϵ in Table I should *not* be construed as descriptive of any actual $\pi\pi$ resonance.

TABLE I. Masses and widths (in MeV) used in phase-space calculations.

Particle[a]	M_0	Γ_0
π	139	
η	549	
ρ	770	153
ϵ	800	800
ω	782	
K	498	
N	939	
Δ	1232	115
N^*	1440	200
Λ	1116	

[a]Values for the ϵ are effective parameters to describe the s-wave isoscalar $\pi\pi$ interaction in the energy range of this analysis. The parameters should not be interpreted as describing an actual $\pi\pi$ resonance (see text).

For the purpose of fitting the $\pi N \to \epsilon N$ amplitudes using two-body unitarity as a constraint, it is important mainly to implement appropriate threshold behavior; the specific values used for the "mass" and "width" of the ϵ are relatively unimportant as long as the mass is ~ 1 GeV and the width is of comparable magnitude.

III. FITTING PROCEDURE

The data fitted by the parametrization discussed in Sec. II consisted of the quasi-two-body $\pi N \to \pi\pi N$ amplitudes from Ref. [1] and the elastic $\pi N \to \pi N$ amplitudes from the Carnegie Mellon–Berkeley (CMB) solution [8] and the Karlsruhe-Helsinki (KH) solution [9]. (The CMB amplitudes, which extend between $W=1.32$ and 2.16 GeV, were supplemented at lower energies by values obtained from a Virginia-Tech analysis [14].) The amplitudes from the CMB and KH analyses were fitted simultaneously in an effort to minimize any bias that might be introduced by fitting either set of amplitudes separately. At energies where differences between the two elastic analyses occurred, the resulting fit was free to agree with the results of one analysis or the other, or with neither.

A nonlinear least-squares algorithm based on the subroutine CURFIT of Bevington [15] was used to determine the fitting parameters; the quantity minimized was χ^2 defined by

$$\chi^2=\sum_i\left[\left[\frac{R_i-T_R(W_i)}{\Delta R_i}\right]^2+\left[\frac{I_i-T_I(W_i)}{\Delta I_i}\right]^2\right]\ . \tag{20}$$

Here R_i and I_i denote the real and imaginary parts of the T-matrix amplitude for the ith data point, respectively, and the quantities $T_R(W_i)$ and $T_I(W_i)$ are the corresponding real and imaginary parts of the parametrization for the T-matrix amplitude evaluated at energy W_i. For the inelastic amplitudes, the uncertainties ΔR_i and ΔI_i were taken from Ref. [1] and typically ranged between ± 0.01 and ± 0.03; uncertainties for the real and imaginary parts of the elastic amplitudes were taken somewhat arbitrarily to be ± 0.015 for c.m. energies up to 50 MeV below the first resonance in a partial wave and were taken to be ± 0.005 at higher energies. All of the inelastic data from Ref. [1] were not included in our fits. Inelastic amplitudes at fixed c.m. energies of 1790 and 1830 MeV were particularly noisy and were omitted for waves with total angular momentum $J \leq \frac{5}{2}$; these amplitudes were based on about half the number of events as were used to determine the amplitudes at adjacent energies.

The partial waves considered in this work are those that have significant inelasticity below about 2 GeV; these include all isospin $I=\frac{1}{2}$ waves with $J \leq \frac{7}{2}$ and all $I=\frac{3}{2}$ waves with initial πN orbital angular momentum $l \leq 3$. To satisfy the unitarity constraint, it was necessary when fitting data for some partial waves to add an inelastic channel for which data were not available. Below about 1600 MeV, ηN (with threshold at $W=1488$ MeV) is the only important inelastic channel other than the various quasi-two-body $\pi\pi N$ channels. At higher energies, other inelastic channels open. (For example, the thresholds for $K\Lambda$ and ωN are 1614 and 1721 MeV, re-

spectively.) Therefore, for resonances with masses greater than about 1600 MeV, the channel added to satisfy unitarity must account for *all* missing inelasticity in the partial wave, not just for the inelasticity associated with the given added channel.

For the S_{11} wave, the obvious channel to add was ηN because of the strong coupling to the $S_{11}(1535)$ resonance, which lies just above η production threshold. For other partial waves, the choice was more arbitrary. We used $K\Lambda$ for the P_{11} wave because the $P_{11}(1710)$ resonance is known to couple strongly to that channel. (The Particle Data Group [10] list $K\Lambda$ and ηN branching fractions of about 15% and 25%, respectively, for the $P_{11}(1710)$; however, the ηN channel cannot account by itself for a small cusplike feature observed in the P_{11} elastic amplitude (see Sec. IV B).) We used ωN for the P_{13} wave because the $P_{13}(1720)$ is near ωN threshold and there is a sharp increase in inelasticity at this energy that cannot be attributed to $\pi\pi N$ channels. We used ηN and ωN for the F_{17} and G_{17} waves, respectively, based in part on theoretical expectations. Finally, we used $\rho\Delta$ for the P_{31}, D_{35}, and F_{37} waves, since this choice seemed reasonable for $I=\frac{3}{2}$ states.

IV. DISCUSSION OF RESONANCE PARAMETERS

Argand diagrams are plotted for each amplitude in Fig. 1 in accordance with the baryon-first convention [1].

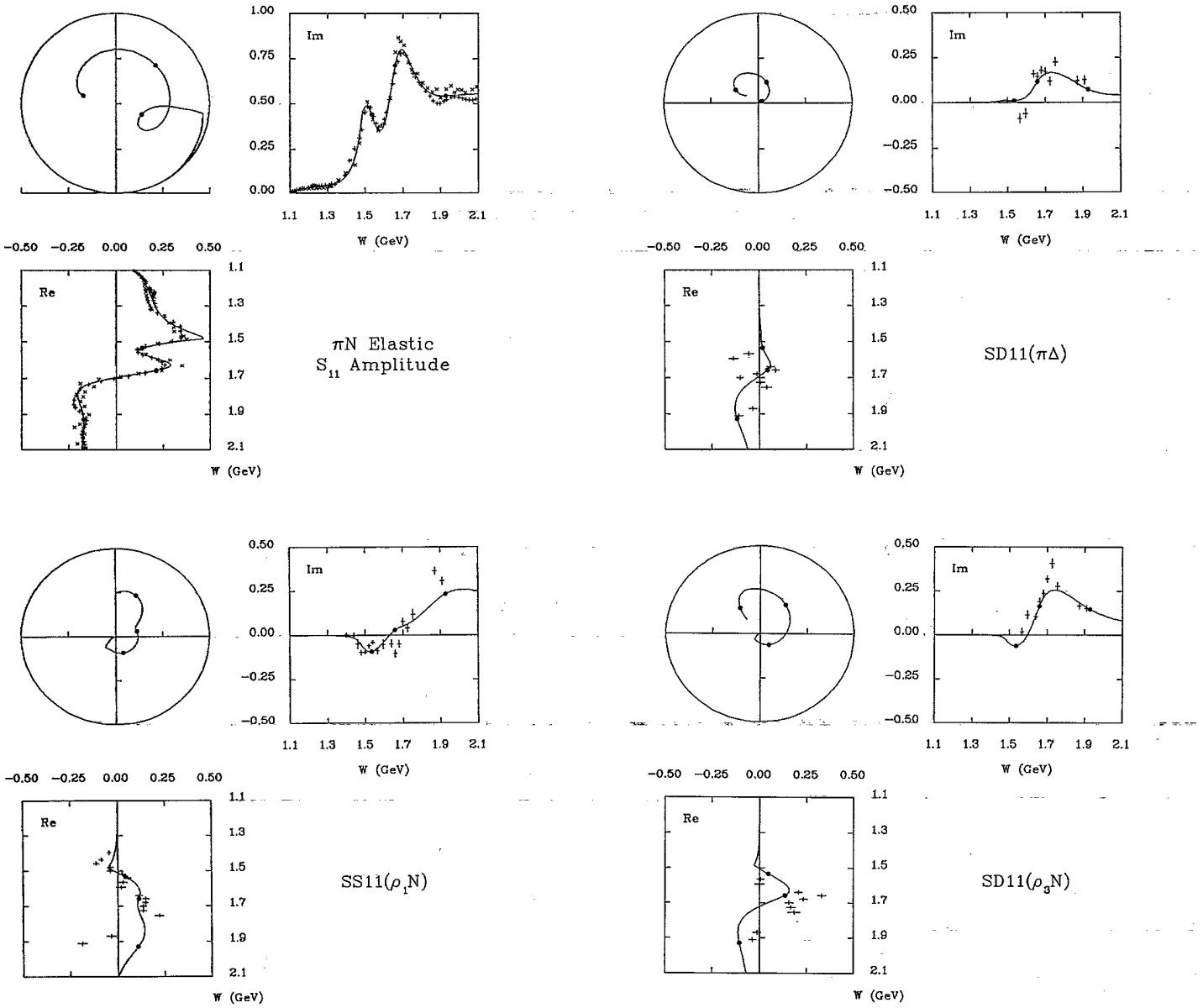

FIG. 1. Argand diagrams for the two-body or quasi-two-body amplitudes. The curves were obtained by fitting all amplitudes for a given partial wave with the unitary parametrization described in the text. Positions of resonances are indicated by small filled circles. All inelastic amplitudes shown are from Ref. [1]; the elastic amplitudes from the CMB [8] and KH [9] analyses are indicated by "×" and "+", respectively.

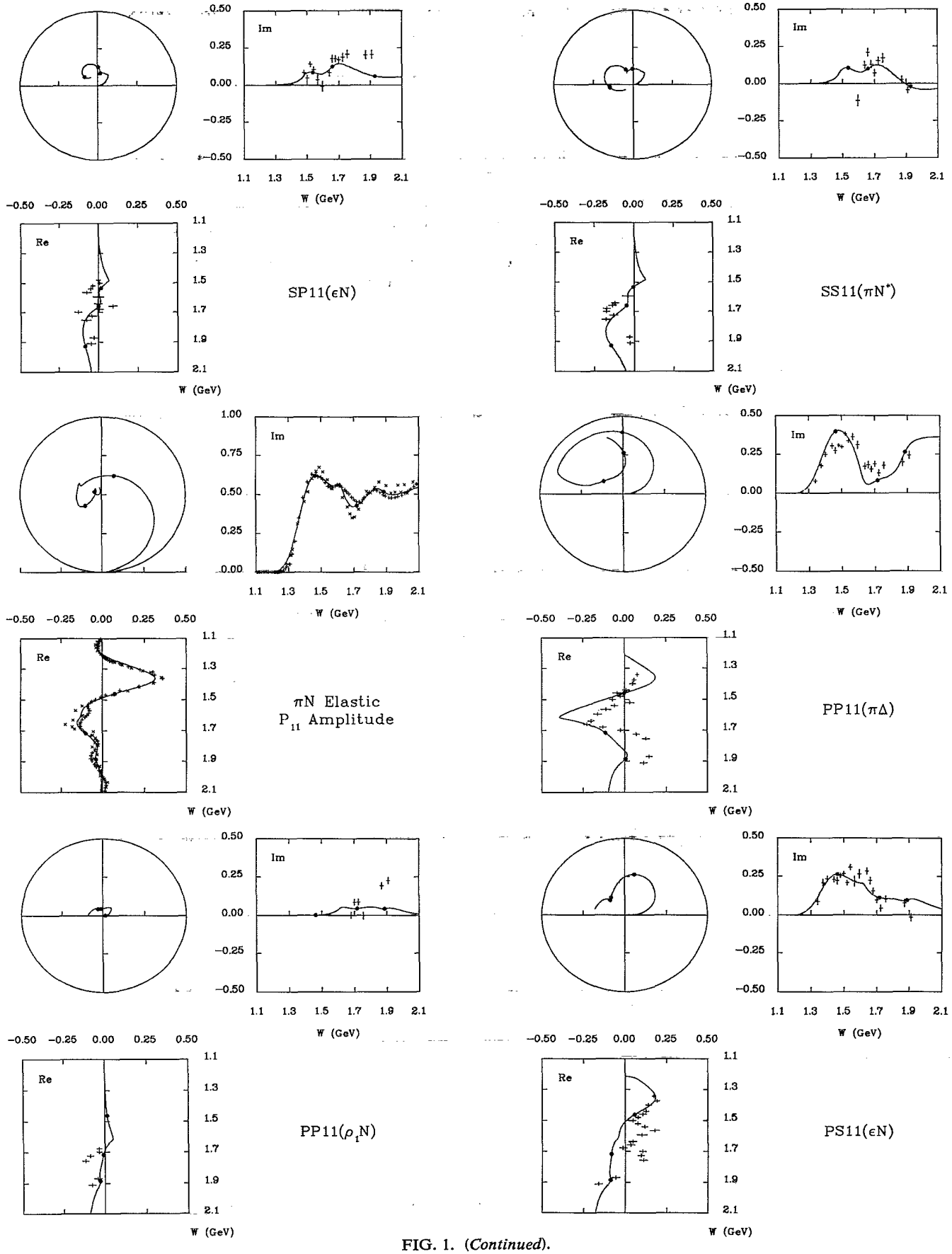

FIG. 1. (*Continued*).

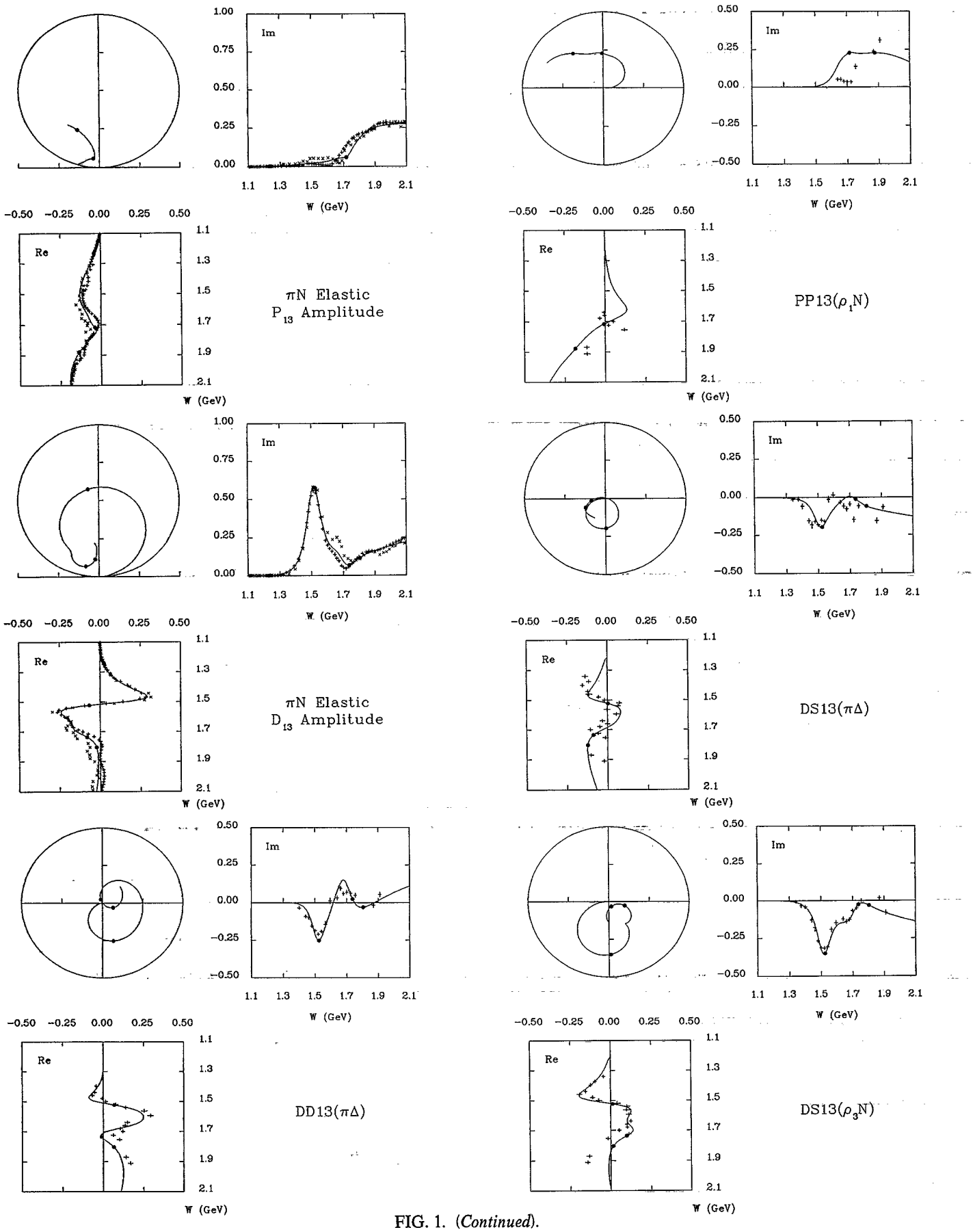

FIG. 1. (*Continued*).

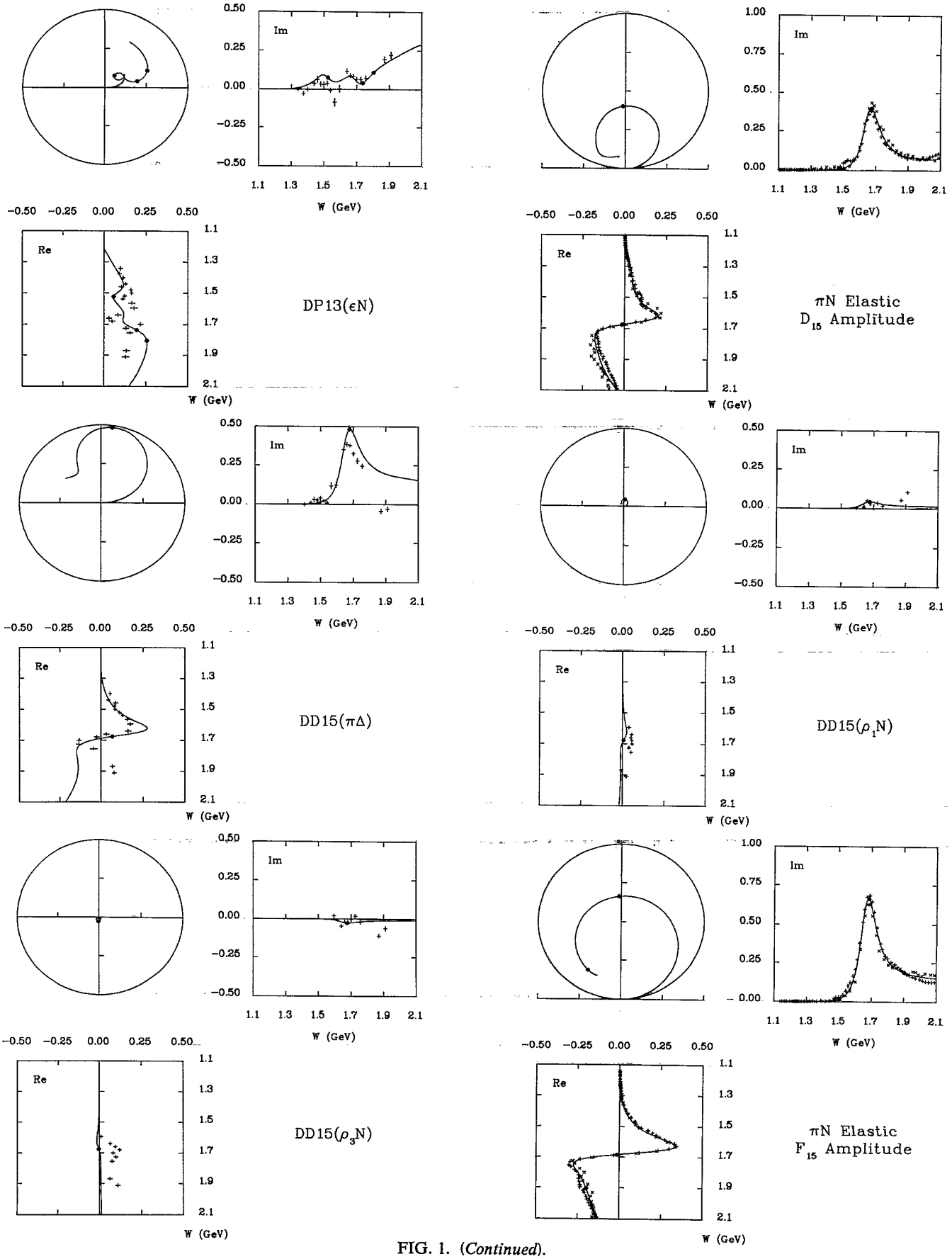

FIG. 1. (*Continued*).

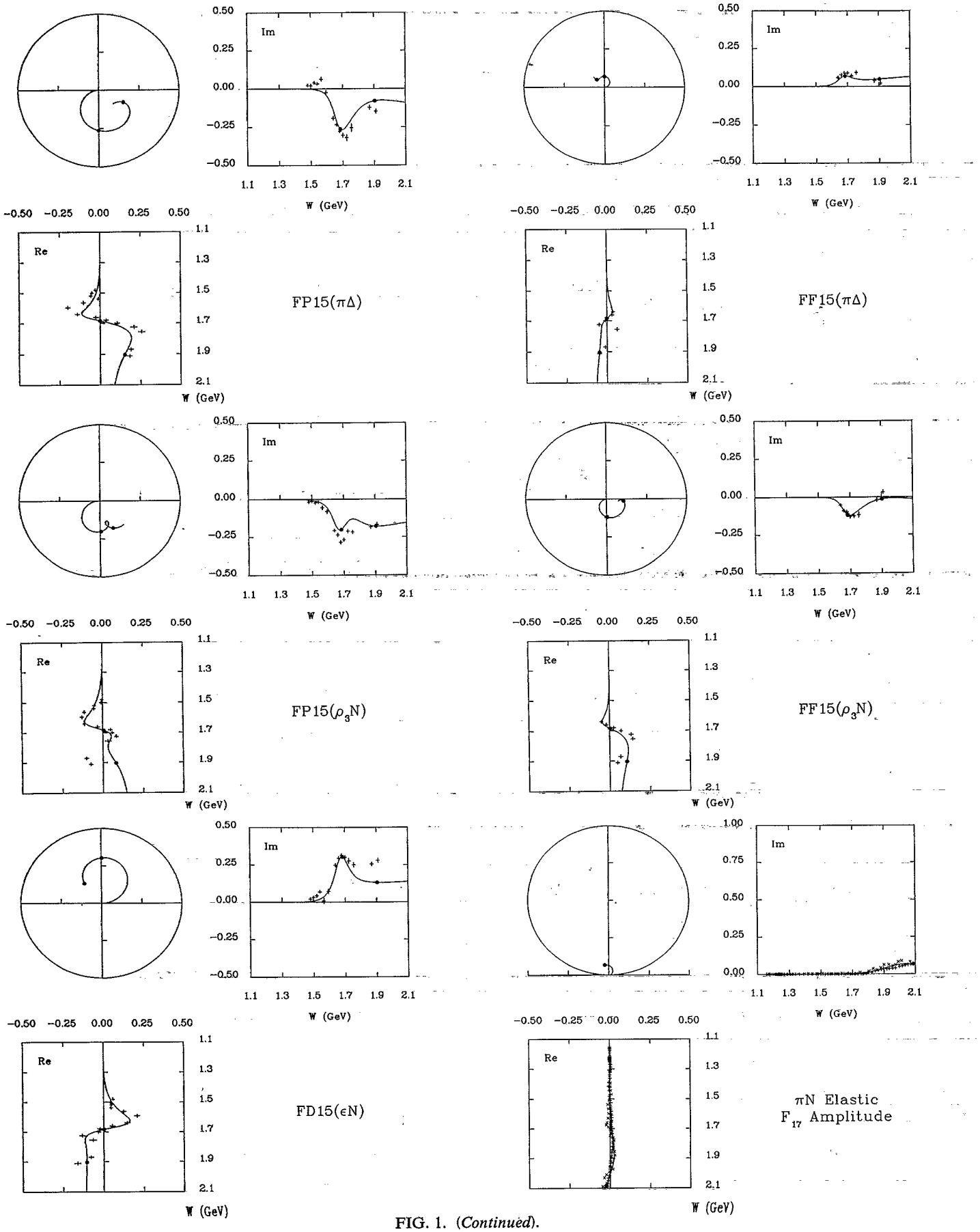

FIG. 1. (*Continued*).

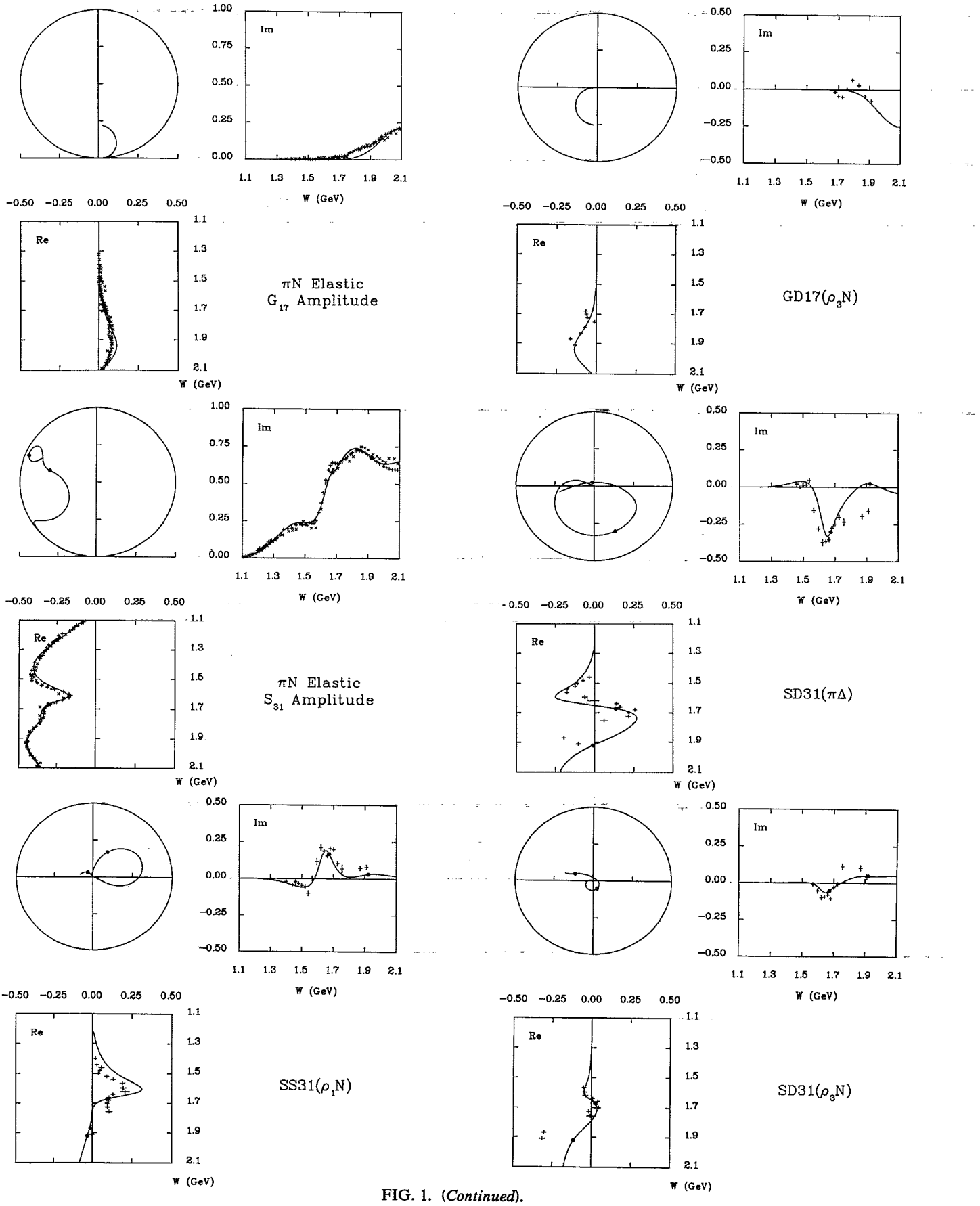

FIG. 1. (*Continued*).

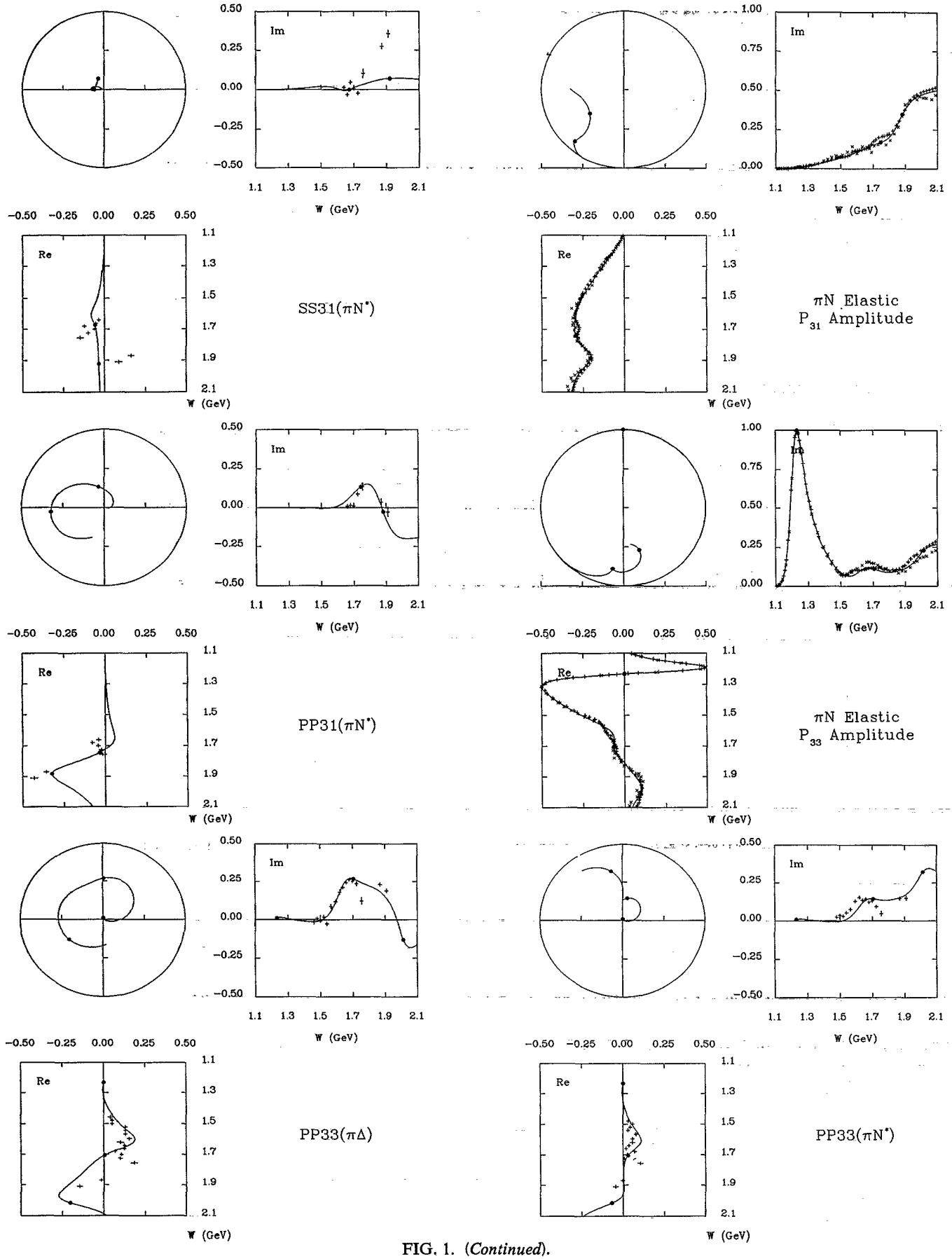

FIG. 1. (*Continued*).

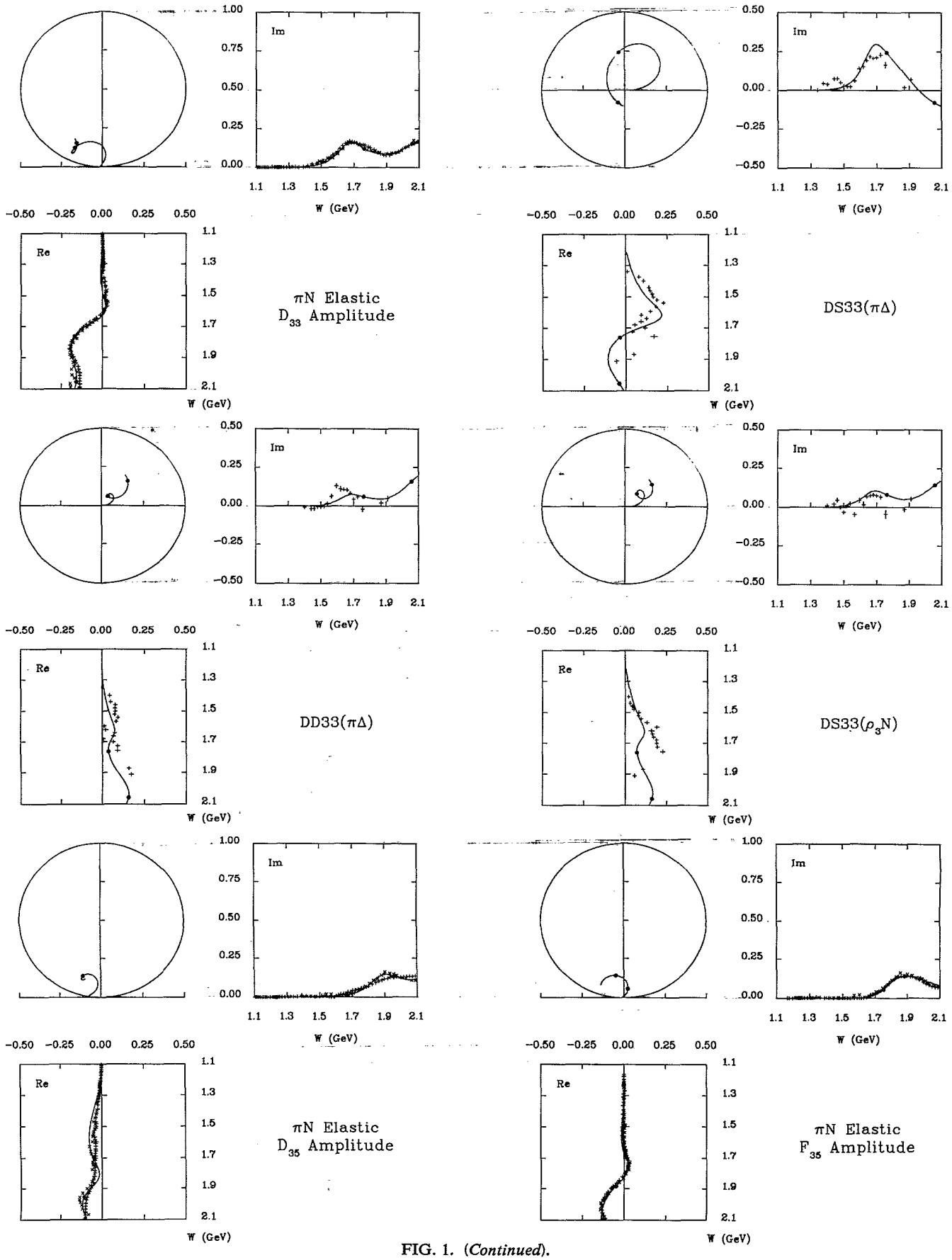

FIG. 1. (*Continued*).

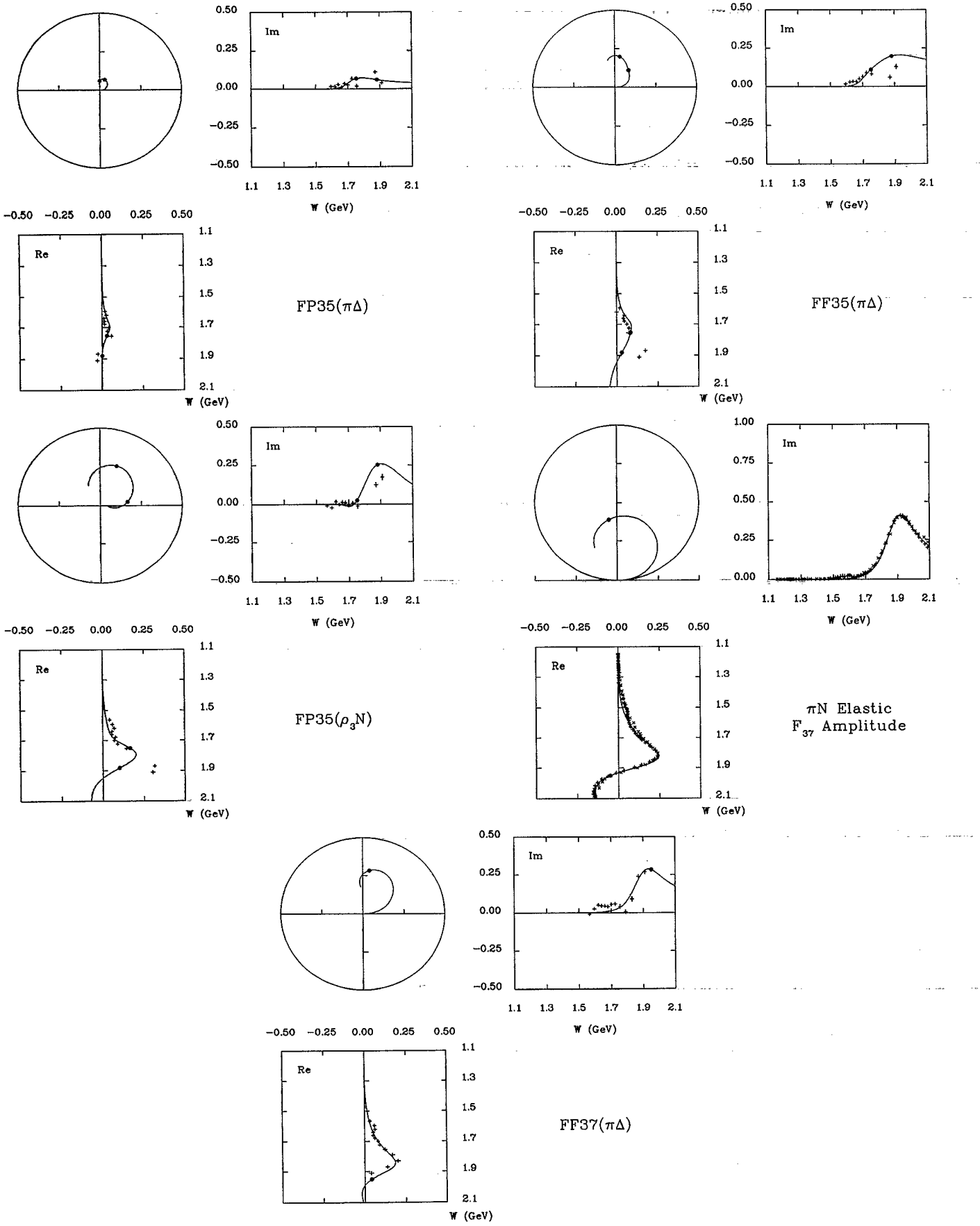

FIG. 1. (*Continued*).

The overall phase ambiguity for $\pi\pi N$ couplings was resolved by choosing a negative sign for the $S_{31}(1620)$ coupling to $\pi\Delta$. Inelastic partial-wave cross sections are plotted for each fitted partial wave in Fig. 2. Curves are shown for both the "total" inelastic partial-wave cross section and for the contribution from decays into $\pi\pi N$ channels (i.e., $\pi\Delta$, ρN, ϵN, πN^*). These curves were generated by fitting the various amplitudes for each partial wave as described in Sec. III. It will be noticed that, in many cases (e.g., F_{37}), the cross sections from the 1980 elastic partial-wave analyses [8,9] show noisy structures or large fluctuations on the low-energy wings of the lowest resonances. This behavior is due to the influence of the tails of high partial waves, which are not well determined by the data [16]. Based on an evaluation of Mandelstam's double spectral function, Höhler *et al.* [17] have derived a suitable theoretical constraint for the inelastic cross sections (for $l \geq 1$) at energies well below the first resonance in the considered partial wave. These constraints were implemented by Koch who used partial-wave dispersion relations and projections of fixed-t dispersion relations to obtain a reasonable smooth threshold behavior of the cross sections [16,18]. The improved Karlsruhe solutions KA84 [16] and KA85 [18] were discussed recently by Höhler [19]. It should also be mentioned that much new and precise data have become available [11] since the 1980 partial-wave analyses. If the new data are compared with predictions from the 1980 CMB and KH solutions, the overall agreement is satisfactory but there are several clear discrepancies [19]. Some corrections to the 1980 CMB and KH solutions are therefore necessary; unfortunately, updating these solutions based on analyticity constraints will require great effort.

Our main results are presented in Tables II and III,

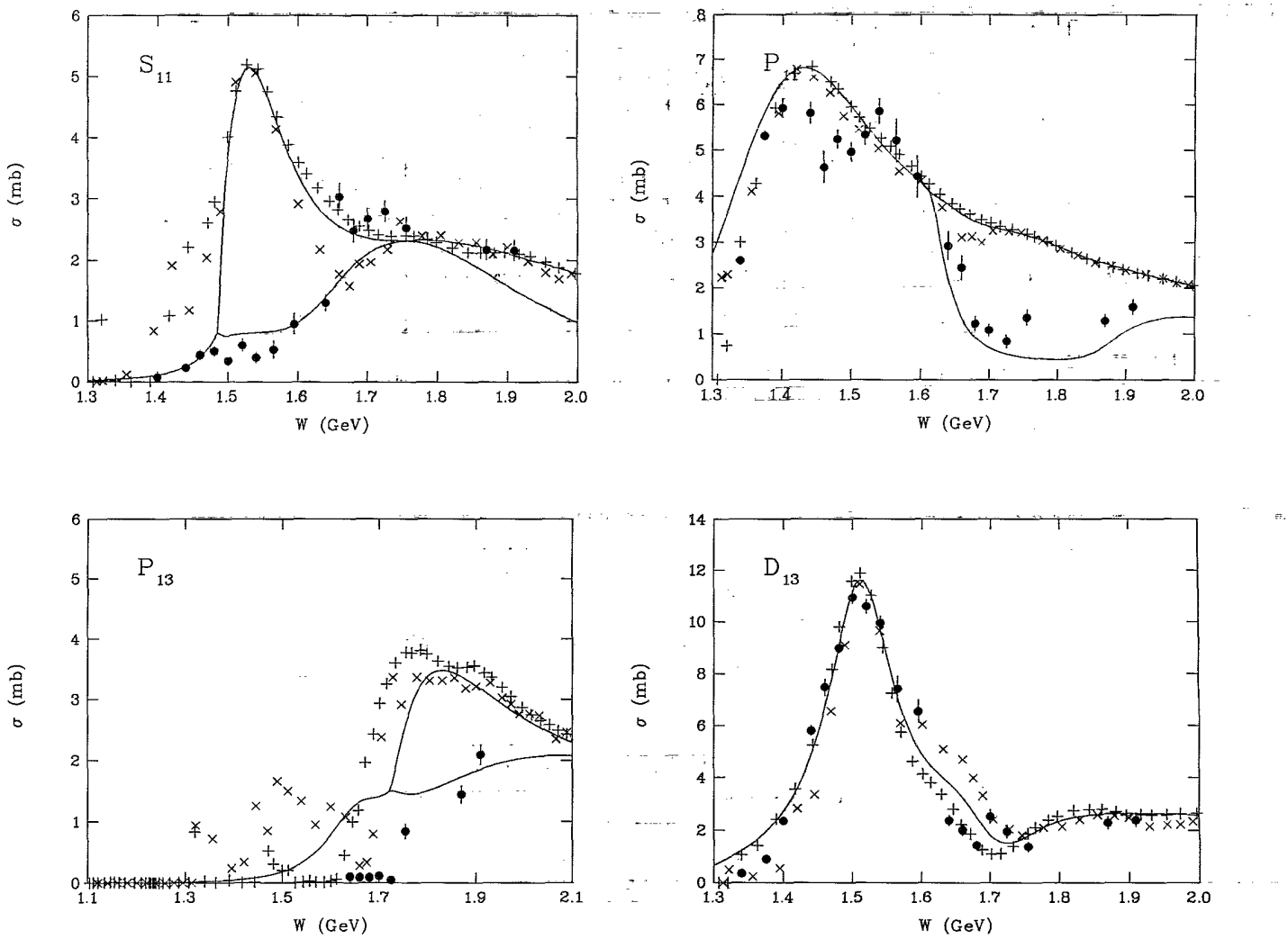

FIG. 2. Inelastic partial-wave cross sections. The results from Ref. [1] showing the contribution to $\pi\pi N$ channels are indicated by small filled circles. The results from the elastic partial-wave analyses of CMB [8] and KH [9] are indicated by "×" and "+", respectively. The curves were obtained by fitting all amplitudes for a given partial wave as described in the text. When two curves are shown, the upper curve represents the total partial-wave cross section and the lower curve represents the contribution from decays into $\pi\pi N$ channels.

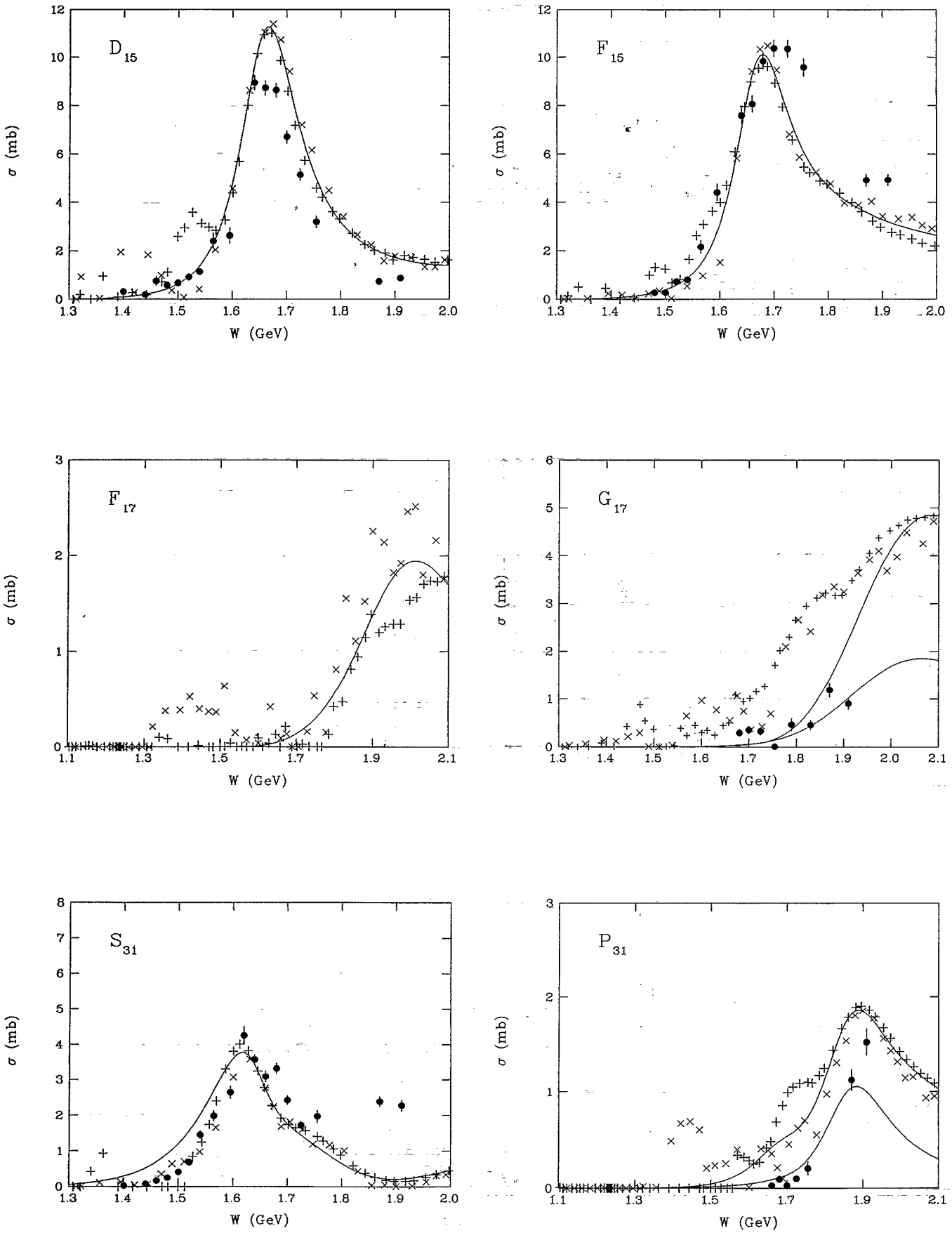

FIG. 2. *(Continued).*

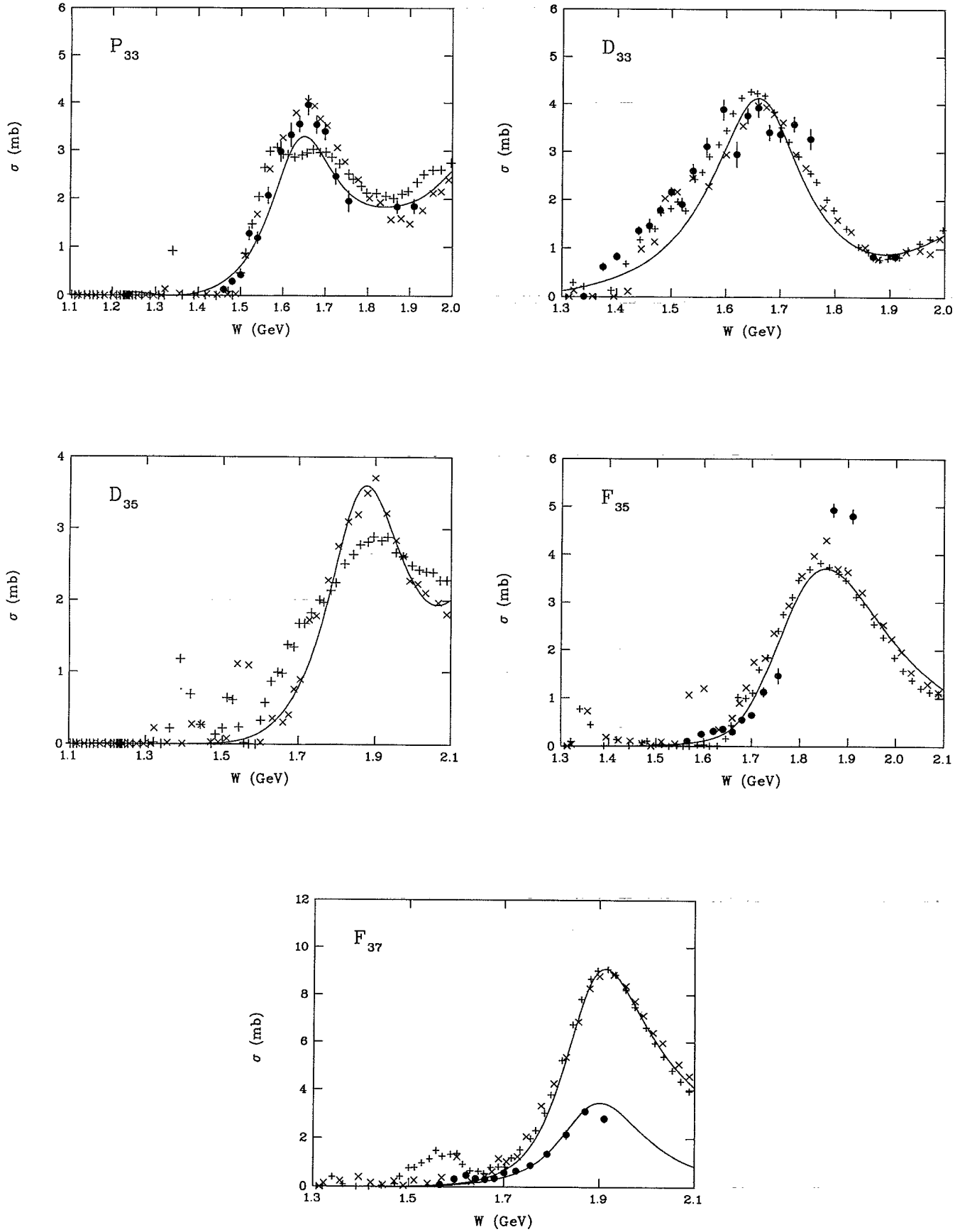

FIG. 2. (*Continued*).

TABLE II. Resonance parameters determined from this work for states with isospin $I=\frac{1}{2}$. (Uncertainties in the last significant figure are given in parentheses.) Resonances are denoted by their nominal mass values taken from the Particle Data Group compilation [10]. A channel subscript for the relative orbital angular momentum is provided in cases that would otherwise be ambiguous.

Resonance mass and width (MeV)	Channel	Partial width (MeV)	Branching fraction (%)	Resonant amplitude
$S_{11}(1535)$	πN	77(17)	51(5)	+0.51(5)
1534(7)	ηN	66(13)	43(6)	+0.47(2)
151(27)	$\pi\Delta$	0(0)	0(0)	+0.00(4)
	$\rho_1 N$	3(2)	2(1)	−0.10(3)
	$\rho_3 N$	2(2)	1(1)	−0.08(3)
	ϵN	1(2)	1(1)	+0.07(4)
	πN^*	3(3)	2(2)	+0.10(5)
$S_{11}(1650)$	πN	154(14)	89(7)	+0.89(7)
1659(9)	ηN	6(8)	3(5)	−0.18(11)
173(12)	$\pi\Delta$	3(2)	2(1)	+0.12(4)
	$\rho_1 N$	0(0)	0(0)	−0.01(9)
	$\rho_3 N$	5(4)	3(2)	+0.16(6)
	ϵN	3(4)	2(2)	+0.12(8)
	πN^*	2(2)	1(1)	+0.11(6)
$S_{11}(2090)$	πN	43(50)	10(10)	+0.10(10)
1928(59)	ηN	2(14)	0(3)	+0.02(8)
414(157)	$\pi\Delta$	26(60)	6(14)	−0.08(8)
	$\rho_1 N$	203(122)	49(22)	+0.22(13)
	$\rho_3 N$	0(4)	0(1)	−0.00(12)
	ϵN	17(41)	4(10)	−0.06(8)
	πN^*	124(97)	30(22)	−0.18(10)
$D_{13}(1520)$	πN	73(6)	59(3)	+0.59(3)
1524(4)	$(\pi\Delta)_S$	7(4)	5(3)	−0.18(5)
124(8)	$(\pi\Delta)_D$	18(5)	15(4)	−0.29(3)
	$(\rho_3 N)_S$	26(6)	21(4)	−0.35(3)
$D_{13}(1700)$	πN	3(7)	1(2)	+0.01(2)
1737(44)	$(\pi\Delta)_S$	12(25)	5(10)	+0.02(3)
249(218)	$(\pi\Delta)_D$	198(158)	80(19)	+0.10(9)
	$(\rho_3 N)_S$	31(63)	13(17)	−0.04(6)
	ϵN	5(10)	2(4)	+0.02(2)
$D_{13}(2080)$	πN	104(40)	23(3)	+0.23(3)
1804(55)	$(\pi\Delta)_S$	15(31)	3(7)	−0.09(9)
447(185)	$(\pi\Delta)_D$	95(82)	21(14)	+0.22(7)
	$(\rho_3 N)_S$	114(75)	26(14)	−0.24(6)
	ϵN	119(73)	27(12)	+0.25(6)
$D_{15}(1675)$	πN	74(4)	47(2)	+0.47(2)
1676(2)	$(\pi\Delta)_D$	84(5)	53(2)	+0.496(3)
159(7)	$\rho_1 N$	0.7(6)	0.4(4)	+0.04(2)
	$(\rho_3 N)_D$	0.3(5)	0.2(3)	−0.03(2)
$G_{17}(2190)$	πN	123(14)	22(1)	+0.22(1)
2127(9)	$(\rho_3 N)_D$	156(30)	29(6)	−0.25(3)
547(48)	$(\omega_3 N)_D$	268(52)	49(7)	−0.33(2)
$P_{11}(1440)$	πN	270(25)	69(3)	+0.69(3)
1462(10)	$\pi\Delta$	88(15)	22(3)	+0.39(2)
391(34)	ϵN	33(10)	9(2)	+0.24(3)

which summarize the resonance parameters for each partial wave with $I=\frac{1}{2}$ and $I=\frac{3}{2}$, respectively. The quoted uncertainties are the values obtained from the fitting procedure multiplied by $(\chi^2/\nu)^{1/2}$ (when $\chi^2/\nu>1$), where ν is the number of degrees of freedom for the fit. No attempt was made to estimate contributions to the total uncertainties resulting from either the model dependency of our parametrization or to specific details of the fitting procedure (e.g., number of resonances or channels included, etc.); thus, the quoted uncertainties generally should be regarded as lower bounds. As discussed in Sec. III, either an ηN, a $K\Lambda$, an ωN, or a $\rho\Delta$ channel was added whenever the total inelasticity was not accounted for by the quasi-two-body $\pi\pi N$ channels. Except for the $S_{11}(1535)$ resonance, the added channel should be regarded only as a reasonable means to satisfy unitarity, and the quoted branching fraction should *not* be interpreted as a true measure of inelasticity in the given channel. For example, the "effective" $K\Lambda$ branching fraction of $(37\pm10)\%$ given in Table II for $P_{11}(1710)$ is consistent with the Particle Data Group [10], who list experimental $K\Lambda$ and ηN branching fractions of about 15% and 25%, respectively, (i.e., the total inelasticity unassociated with $\pi\pi N$ channels is about 40%).

In Table IV, the masses, widths, and elasticities (elastic branching fractions) determined by this analysis (KSU) for $I=\frac{1}{2}$ resonances are compared with those of the CMB [8] and KH [9] elastic phase-shift analyses; a similar comparison is presented in Table V for $I=\frac{3}{2}$ resonances. (The recent elastic analysis of Arndt *et al.* [11] quotes pole positions rather than Breit-Wigner masses and widths.) The KSU, CMB, and KH analyses are expected to agree best for those resonances with large (>40%) elastic branching fractions; all three analyses agree that this property is shared by $P_{33}(1232)$, $P_{11}(1440)$, $D_{13}(1520)$, $S_{11}(1535)$, $S_{11}(1650)$, $D_{15}(1675)$,

TABLE II. (*Continued*).

Resonance mass and width (MeV)	Channel	Partial width (MeV)	Branching fraction (%)	Resonant amplitude
$P_{11}(1710)$	πN	45(22)	9(4)	+0.09(4)
1717(28)	$\pi\Delta$	234(110)	49(10)	−0.21(4)
478(226)	$\rho_1 N$	15(34)	3(7)	+0.05(6)
	ϵN	10(19)	2(4)	+0.04(5)
	$K\Lambda$	175(106)	37(10)	−0.19(4)
$P_{11}(2100)$	πN	17(11)	15(6)	+0.15(6)
1885(30)	$\pi\Delta$	28(21)	24(18)	−0.19(8)
113(44)	$\rho_1 N$	30(91)	27(79)	+0.20(30)
	ϵN	36(82)	32(71)	+0.22(25)
	$K\Lambda$	3(7)	2(6)	−0.06(7)
$P_{13}(1720)$	πN	50(16)	13(5)	+0.13(5)
1717(31)	$\rho_1 N$	333(168)	87(5)	+0.34(5)
383(179)				
P_{13}	πN	130(37)	26(6)	+0.26(6)
1879(17)	$\rho_1 N$	217(87)	44(15)	−0.34(3)
498(78)	$\omega_1 N$	151(45)	30(10)	+0.28(7)
$F_{15}(1680)$	πN	96(6)	70(3)	+0.70(3)
1684(4)	$(\pi\Delta)_P$	13(4)	10(3)	−0.26(4)
139(8)	$(\pi\Delta)_F$	1(1)	1(1)	+0.07(3)
	$(\rho_3 N)_P$	8(4)	5(3)	−0.20(5)
	$(\rho_3 N)_F$	3(2)	2(1)	−0.13(3)
	ϵN	17(5)	12(3)	+0.29(4)
$F_{15}(2000)$	πN	39(33)	8(5)	+0.08(5)
1903(87)	$(\pi\Delta)_P$	60(90)	12(17)	+0.10(6)
494(308)	$(\pi\Delta)_F$	2(26)	0(5)	+0.02(11)
	$(\rho_3 N)_P$	296(212)	60(23)	−0.22(8)
	$(\rho_3 N)_F$	73(99)	15(17)	+0.11(6)
	ϵN	24(56)	5(11)	+0.06(8)
$F_{17}(1990)$	πN	34(18)	6(2)	+0.06(2)
2086(28)	ηN	501(102)	94(2)	−0.24(4)
535(117)				

TABLE III. Resonance parameters determined from this work for states with isospin $I = \frac{3}{2}$. (Uncertainties in the last significant figure are given in parentheses). Resonances are denoted by their nominal mass values taken from the Particle Data Group compilation [10]. A channel subscript for the relative orbital angular momentum is provided in cases that would otherwise be ambiguous.

Resonance mass and width (MeV)	Channel	Partial width (MeV)	Branching fraction (%)	Resonant amplitude
$S_{31}(1620)$	πN	14(6)	9(2)	+0.09(2)
1672(7)	$\pi\Delta$	95(25)	62(6)	−0.24(3)
154(37)	$\rho_1 N$	38(11)	25(6)	+0.15(2)
	$\rho_3 N$	6(1)	4(3)	−0.06(2)
$S_{31}(1900)$	πN	107(22)	41(4)	+0.41(4)
1920(24)	$\pi\Delta$	41(24)	16(8)	+0.25(7)
263(39)	$\rho_1 N$	12(19)	5(7)	−0.14(11)
	$\rho_3 N$	86(32)	33(10)	−0.37(7)
	πN^*	17(23)	6(9)	−0.16(11)
$D_{33}(1700)$	πN	81(34)	14(6)	+0.14(6)
1762(44)	$(\pi\Delta)_S$	445(200)	74(7)	+0.32(6)
599(248)	$(\pi\Delta)_D$	26(22)	4(3)	+0.08(3)
	$(\rho_3 N)_S$	46(31)	8(4)	+0.10(3)
$D_{33}(1940)$	πN	81(104)	18(12)	+0.18(12)
2057(110)	$(\pi\Delta)_S$	30(69)	7(15)	+0.11(10)
460(316)	$(\pi\Delta)_D$	187(212)	41(32)	+0.27(16)
	$(\rho_3 N)_S$	162(143)	35(31)	+0.25(10)
$D_{35}(1930)$	πN	93(24)	18(2)	+0.18(2)
1956(22)	$(\rho_1\Delta)_D$	433(122)	82(2)	−0.38(2)
526(142)				
$D_{35}(2350)$	πN	5(2)	2.0(3)	+0.020(3)
2171(18)	$(\rho_1\Delta)_D$	259(50)	98.0(3)	+0.14(1)
264(51)				
P_{31}	πN	24(13)	8(3)	+0.08(3)
1744(36)	πN^*	84(58)	28(9)	+0.15(3)
299(118)	$(\rho_1\Delta)_P$	191(53)	64(9)	−0.23(5)
$P_{31}(1910)$	πN	55(22)	23(8)	+0.23(8)
1882(10)	πN^*	159(21)	67(10)	−0.39(4)
239(25)	$(\rho_1\Delta)_P$	24(11)	10(4)	+0.15(5)
$P_{33}(1232)$	πN	118(4)	100	+1.00
1231(1)	$(\pi\Delta)_P$	0.01(2)	0.01(1)	+0.011(6)
118(4)	πN^*	0.01(2)	0.01(1)	+0.008(8)
$P_{33}(1600)$	πN	53(9)	12(2)	+0.12(2)
1706(10)	$(\pi\Delta)_P$	290(53)	67(5)	+0.29(2)
430(73)	πN^*	87(27)	20(4)	+0.16(2)
$P_{33}(1920)$	πN	3(4)	2(2)	+0.02(2)
2014(16)	$(\pi\Delta)_P$	126(38)	83(26)	−0.13(4)
152(55)	πN^*	23(42)	15(24)	+0.06(7)
F_{35}	πN	4(3)	2(1)	+0.02(1)
1752(32)	$(\pi\Delta)_P$	71(60)	28(18)	+0.07(3)
251(93)	$(\pi\Delta)_F$	121(64)	48(16)	+0.09(4)
	$(\rho_3 N)_P$	55(28)	22(14)	−0.06(1)

TABLE III. (*Continued*).

Resonance mass and width (MeV)	Channel	Partial width (MeV)	Branching fraction (%)	Resonant amplitude
$F_{35}(1905)$	πN	41(13)	12(3)	+0.12(3)
1881(18)	$(\pi\Delta)_P$	4(10)	1(3)	−0.04(5)
327(51)	$(\pi\Delta)_F$	2(4)	0(1)	+0.02(3)
	$(\rho_3 N)_P$	282(42)	86(3)	+0.33(3)
$F_{37}(1950)$	πN	114(2)	38(1)	+0.38(1)
1945(2)	$(\pi\Delta)_F$	55(10)	18(3)	+0.27(2)
300(7)	$(\rho_3\Delta)_F$	130(11)	43(3)	+0.41(2)

$F_{15}(1680)$, and $F_{37}(1950)$. The masses and elasticities that we determined for all of these resonances agree reasonably well with the results of both elastic analyses. The total widths determined by our analysis for $P_{33}(1232)$, $D_{13}(1520)$, $S_{11}(1650)$, and $F_{15}(1680)$ also agree reasonably well with both elastic analyses. The total widths determined by our analysis for $P_{11}(1440)$, $D_{15}(1675)$, and $F_{37}(1950)$ agree better with the results of the CMB analysis than with those of the KH analysis, which found smaller widths for each state. This situation probably can be understood from the fact that the KH parametrization included only a single resonance with fitting performed only in the near vicinity of the resonances while both the KSU and CMB parametrizations included multiple resonances with fitting performed over an extended energy range. Additional differences between the KH and CMB analyses and resonance parameters have been discussed by Höhler [20].

A detailed comparison between several analyses of the relative *signs* of resonant couplings was presented in Ref. [1]; here, we give an updated, more complete comparison by presenting values of the resonant amplitudes determined by this analysis (KSU) and those of Ref. [2] (Saclay), Ref. [3] (LBL-SLAC), and Ref. [21] [Imperial College (IC)]. In the present work, the resonant amplitudes are given by Eq. (12) evaluated at $W=m_k$, where m_k is the mass of the kth resonance. (The IC amplitudes were determined by an Imperial College group who analyzed $\pi^+ p$ events; hence, these amplitudes furnish information only about $I=\frac{3}{2}$ resonances.) Resonant $\pi N\to\pi\Delta$ amplitudes are compared in Table VI, resonant $\pi N\to\rho N$ amplitudes are compared in Table VII, and resonant $\pi N\to\epsilon N$ amplitudes are compared in Table VIII.

The constituent quark model provides a convenient classification scheme for light baryons in terms of a flavor-spin SU(6) basis. In several cases, physical states belong to a dominant SU(6) supermultiplet specified by (D,L_N^P), where D is the dimensionality of the representation, L is the total quark orbital angular momentum, and $P=(-1)^N$ is the total parity. Here N is the number of quanta of unperturbed excitation energy. The $N=0$ band consists only of the $(56,0_0^+)$ supermultiplet, which contains the nucleon $P_{11}(939)$ and the lowest-mass Δ resonance $P_{33}(1232)$. In the present work, we find the first P_{33} resonance at 1231±1 MeV with a width of 118±4 MeV; these values are determined essentially from the elastic amplitudes and agree well with the values of CMB and KH (see Table V). (Note that values for the $P_{33}(1232)$ are presented primarily as a check of our fitting procedure and for completeness. Similarly, we include results for the F_{17} and D_{35} waves, even though the $\pi\pi N$ inelasticities were too small to determine meaningful $\pi N\to\pi\pi N$ amplitudes for these waves [1].)

A. Low-lying negative-parity states

The $N=1$ band consists only of the $(70,1_1^-)$ supermultiplet. It contains $S_{11}(1535)$ and $D_{13}(1520)$, which are states mainly with total quark spin $S=\frac{1}{2}$, and $S_{11}(1650)$, $D_{13}(1700)$, and $D_{15}(1675)$, which are states mainly with $S=\frac{3}{2}$. This band also contains $S_{31}(1620)$ and $D_{33}(1700)$, which mainly have $S=\frac{1}{2}$. Our results for these states are discussed below.

$S_{11}(1535)$. We find the lowest S_{11} resonance at 1534±7 MeV with a width of 151±27 MeV. These values are consistent, within uncertainties, with both CMB and KH (see Table IV). The present work determines the πN branching fraction to be (51±5)%. Its couplings to $\pi\Delta$ and ρN are small; our values are consistent with those of Saclay and LBL-SLAC. The most striking feature of this state is its well-known strong coupling to ηN. This coupling is responsible for the strong cusp evident in the elastic amplitude and less evident in the inelastic amplitudes. (See the S_{11} Argand diagrams in Fig. 1. Note that the same coupling is responsible for the cusp in the inelastic S_{11} cross section visible in Fig. 2.) In the present work, ηN is the most important *inelastic* decay mode, with a branching fraction of (43±6)%.

$D_{13}(1520)$. We find the lowest D_{13} resonance at 1524±4 MeV with a width of 124±8 MeV. These values are consistent with both CMB and KH. It has large negative couplings to $(\pi\Delta)_S$ and $(\pi\Delta)_D$. Our $\pi\Delta$ couplings agree reasonably with both Saclay and LBL-SLAC, although the agreement is slightly better with LBL-SLAC. This state also has a large negative coupling to $(\rho_3 N)_S$. Our $(\rho_3 N)_S$ coupling is in good agreement with the Saclay value but only in fair agreement with the LBL-

TABLE IV. Resonance parameters (masses, widths, and elasticities) for $I=\frac{1}{2}$ states determined by the present work (KSU) compared with those determined from the CMB [8] and KH [9] elastic phase-shift analyses. When possible, each resonance is denoted (first column) by its nominal mass and status taken from the PDG [10].

Resonance	Mass (MeV)	Width (MeV)	Elasticity	Reference
$S_{11}(1535)$	1534(7)	151(27)	0.51(5)	KSU
****	1526(7)	120(20)	0.38(4)	KH
	1550(40)	240(80)	0.50(10)	CMB
$S_{11}(1650)$	1659(9)	173(12)	0.89(7)	KSU
****	1670(8)	180(20)	0.61(4)	KH
	1650(30)	150(40)	0.65(10)	CMB
$S_{11}(2090)$	1928(59)	414(157)	0.10(10)	KSU
*	1880(20)	95(30)	0.09(5)	KH
	2180(80)	350(100)	0.18(8)	CMB
$D_{13}(1520)$	1524(4)	124(8)	0.59(3)	KSU
****	1519(4)	114(7)	0.54(3)	KH
	1525(10)	120(15)	0.58(3)	CMB
$D_{13}(1700)$	1737(44)	249(218)	0.01(2)	KSU
***	1731(15)	110(30)	0.08(3)	KH
	1675(25)	90(40)	0.11(5)	CMB
$D_{13}(2080)$	1804(55)	104(40)	0.23(3)	KSU
**	2081(20)	265(40)	0.06(2)	KH
	1880(100)	180(60)	0.10(4)	CMB
	2060(80)	300(100)	0.14(7)	CMB
$D_{15}(1675)$	1676(2)	159(7)	0.47(2)	KSU
***	1679(8)	120(15)	0.38(3)	KH
	1675(10)	160(20)	0.38(5)	CMB
$G_{17}(2190)$	2127(9)	547(48)	0.22(1)	KSU
****	2140(12)	390(30)	0.14(2)	KH
	2200(70)	500(150)	0.12(6)	CMB
$P_{11}(1440)$	1462(10)	391(34)	0.69(3)	KSU
****	1410(12)	135(10)	0.51(5)	KH
	1440(30)	340(70)	0.68(4)	CMB
$P_{11}(1710)$	1717(28)	478(226)	0.09(4)	KSU
***	1723(9)	120(15)	0.12(4)	KH
	1700(50)	90(30)	0.20(4)	CMB
$P_{11}(2100)$	1885(30)	113(44)	0.15(6)	KSU
*	2050(20)	200(30)	0.10(4)	KH
	2125(75)	260(100)	0.12(3)	CMB
$P_{13}(1720)$	1717(31)	383(179)	0.13(5)	KSU
****	1710(20)	190(30)	0.14(3)	KH
	1700(50)	125(70)	0.10(4)	CMB
P_{13}	1879(17)	498(78)	0.26(6)	KSU
$F_{15}(1680)$	1684(4)	139(8)	0.70(3)	KSU
****	1684(3)	128(8)	0.65(2)	KH
	1680(10)	120(10)	0.62(5)	CMB
$F_{15}(2000)$	1903(87)	494(308)	0.08(5)	KSU
**	1882(10)	95(20)	0.04(2)	KH
$F_{17}(1990)$	2086(28)	535(117)	0.06(2)	KSU
**	2005(150)	350(100)	0.04(2)	KH
	1970(50)	350(120)	0.06(2)	CMB

SLAC value. The resonance parameters for this state are determined well and consistently by all of the major analyses.

$S_{31}(1620)$. We find the lowest S_{31} resonance at 1672±7 MeV, which is perhaps as much as 50 MeV *higher* than CMB and KH (see Table V). The width is 154±37 MeV, which is consistent with CMB and KH. What is striking about this state compared to those discussed already is that, at energies below the first resonance, the S_{31} wave is strongly *repulsive,* as indicated by

TABLE V. Resonance parameters (masses, widths, and elasticities) for $I=\frac{3}{2}$ states determined by the present work (KSU) compared with those determined from the CMB [8] and KH [9] elastic phase-shift analyses. When possible, each resonance is donated (first column) by its nominal mass and status taken from the PDG [10].

Resonance	Mass (MeV)	Width (MeV)	Elasticity	Reference
$S_{31}(1620)$	1672(7)	154(37)	0.09(2)	KSU
****	1610(7)	139(18)	0.35(6)	KH
	1620(20)	140(20)	0.25(3)	CMB
$S_{31}(1900)$	1920(24)	263(39)	0.41(4)	KSU
***	1908(30)	140(40)	0.08(4)	KH
	1890(50)	170(50)	0.10(3)	CMB
$D_{33}(1700)$	1762(44)	599(248)	0.14(6)	KSU
****	1680(70)	230(80)	0.20(3)	KH
	1710(30)	280(80)	0.12(3)	CMB
$D_{33}(1940)$	2057(110)	460(316)	0.18(2)	KSU
*	1940(100)	200(100)	0.05(2)	CMB
$D_{35}(1930)$	1956(22)	526(142)	0.18(2)	KSU
***	1901(15)	195(60)	0.04(3)	KH
	1940(30)	320(60)	0.14(4)	CMB
$D_{35}(2350)$	2171(18)	264(51)	0.020(3)	KSU
*	2305(26)	300(70)	0.04(2)	KH
	2400(125)	400(150)	0.20(10)	CMB
P_{31}	1744(36)	299(118)	0.08(3)	KSU
$P_{31}(1910)$	1882(10)	239(25)	0.23(8)	KSU
****	1888(20)	280(50)	0.24(6)	KH
	1910(40)	225(50)	0.19(3)	CMB
$P_{33}(1232)$	1231(1)	118(4)	1.00	KSU
****	1233(2)	116(5)	1.00	KH
	1232(3)	120(5)	1.00	CMB
$P_{33}(1600)$	1706(10)	430(73)	0.12(2)	KSU
**	1522(13)	220(40)	0.21(6)	KH
	1600(50)	300(100)	0.18(4)	CMB
$P_{33}(1920)$	2014(16)	152(55)	0.02(2)	KSU
***	1868(10)	220(80)	0.14(4)	KH
	1920(80)	300(100)	0.20(5)	CMB
F_{35}	1752(32)	251(93)	0.02(1)	KSU
$F_{35}(1905)$	1881(18)	327(51)	0.12(3)	KSU
****	1905(20)	260(20)	0.15(2)	KH
	1910(30)	400(100)	0.08(3)	CMB
$F_{37}(1950)$	1945(2)	300(7)	0.38(1)	KSU
****	1913(8)	224(10)	0.38(2)	KH
	1950(15)	340(50)	0.39(4)	CMB

TABLE VI. Resonant $\pi N \to \pi\Delta$ amplitudes determined from the Saclay [2], Berkeley-Stanford (LBL-SLAC) [3], Imperial College (IC) [21], and present (KSU) analyses. Resonances are denoted by their nominal mass values taken from the PDG [10]. Well-determined amplitudes with consistent values are denoted by an asterisk.

Amplitude	Mass (MeV)	Saclay	LBL-SLAC	IC	KSU
$SD11(\pi\Delta)$	1535	0.00	+0.06		+0.00(4)
* $SD11(\pi\Delta)$	1650	+0.29	+0.15		+0.12(4)
* $DS13(\pi\Delta)$	1520	−0.26	−0.24		−0.18(5)
* $DD13(\pi\Delta)$	1520	−0.21	−0.30		−0.29(3)
$DS13(\pi\Delta)$	1700	0.00	−0.16		+0.02(3)
$DD13(\pi\Delta)$	1700	−0.12	+0.14		+0.10(9)
* $DD15(\pi\Delta)$	1675	+0.46	+0.50		+0.496(3)
* $PP11(\pi\Delta)$	1440	+0.41	+0.37		+0.39(2)
$PP11(\pi\Delta)$	1710	−0.17	+0.20		−0.21(4)
$PP13(\pi\Delta)$	1710	−0.17			
* $FP15(\pi\Delta)$	1680	−0.27	−0.25		−0.26(4)
* $FF15(\pi\Delta)$	1680	+0.07	+0.08		+0.07(3)
* $SD31(\pi\Delta)$	1620	−0.39	−0.40	−0.33(6)	−0.24(3)
* $DS33(\pi\Delta)$	1700	+0.30	+0.24	+0.18(4)	+0.32(6)
* $DD33(\pi\Delta)$	1700	+0.05	+0.10	±0.14(4)	+0.08(3)
$PP31(\pi\Delta)$	1910	+0.06			
* $PP33(\pi\Delta)$	1600	+0.34	+0.30	+0.24(5)	+0.29(2)
$FP35(\pi\Delta)$	1905				−0.04(5)
$FF35(\pi\Delta)$	1905		+0.20		+0.02(3)
* $FF37(\pi\Delta)$	1950		+0.32		+0.27(2)

TABLE VII. Resonant $\pi N \to \rho N$ amplitudes determined from the Saclay [2], Berkeley-Stanford (LBL-SLAC) [3], Imperial College (IC) [21], and present (KSU) analyses. Resonances are denoted by their nominal mass values taken from the PDG [10]. Well-determined amplitudes with consistent values are denoted by an asterisk.

Amplitude	Mass (MeV)	Saclay	LBL-SLAC	IC	KSU
* $SS11(\rho_1 N)$	1535	−0.10	−0.09		−0.10(3)
$SD11(\rho_3 N)$	1535				−0.08(3)
$SS11(\rho_1 N)$	1650	+0.17	−0.16		−0.01(9)
$SD11(\rho_3 N)$	1650	+0.29			+0.16(6)
* $DS13(\rho_3 N)$	1520	−0.35	−0.24		−0.35(3)
$DS13(\rho_3 N)$	1700	−0.07	+0.07		−0.04(6)
$DD15(\rho_1 N)$	1675				+0.04(2)
$DD15(\rho_3 N)$	1675	−0.15			−0.03(2)
$GD17(\rho_3 N)$	2190				−0.25(3)
$PP11(\rho_1 N)$	1440	−0.11	+0.23		
$PP11(\rho_3 N)$	1440	+0.18			
$PP11(\rho_1 N)$	1710	+0.19	−0.20		+0.05(6)
$PP11(\rho_3 N)$	1710	+0.31			
$PP13(\rho_1 N)$	1720	−0.26	+0.40		+0.34(5)
$PP13(\rho_3 N)$	1720	+0.15			
* $FP15(\rho_3 N)$	1680	−0.23	−0.30		−0.20(5)
* $FF15(\rho_3 N)$	1680	−0.15			−0.13(3)
* $SS31(\rho_1 N)$	1620	+0.08	+0.28	+0.40(10)	+0.15(2)
$SD31(\rho_3 N)$	1620	−0.13			−0.06(2)
$DD33(\rho_1 N)$	1700			+0.17(5)	
$DS33(\rho_3 N)$	1700	+0.04	−0.30		+0.10(3)
$DD33(\rho_3 N)$	1700			±0.18(7)	
$PP31(\rho_1 N)$	1910	+0.29			
$PP33(\rho_1 N)$	1600	+0.10			
$PP33(\rho_3 N)$	1600	+0.10			
* $FP35(\rho_3 N)$	1905		+0.33		+0.33(3)
$FF37(\rho_3 N)$	1950		+0.24		

TABLE VIII. Resonant $\pi N \to \epsilon N$ amplitudes determined from the Saclay [2], Berkeley-Stanford (LBL-SLAC) [3], and present (KSU) analyses. Resonances are denoted by their nominal mass values taken from the PDG [10]. Well-determined amplitudes with consistent values are denoted by an asterisk.

Amplitude	Mass (MeV)	Saclay	LBL-SLAC	KSU
* $SP11(\epsilon N)$	1535	+0.08	+0.09	+0.07(4)
$SP11(\epsilon N)$	1650	0.00	+0.25	+0.12(8)
$DP13(\epsilon N)$	1520	−0.13	−0.17	+0.00(6)
$DP13(\epsilon N)$	1700	0.00	+0.2	+0.02(2)
$DF15(\epsilon N)$	1675	+0.03		
$PS11(\epsilon N)$	1440	−0.18	−0.23	+0.24(3)
$PS11(\epsilon N)$	1710	−0.26	−0.28	+0.04(5)
$PD13(\epsilon N)$	1720	−0.19		
* $FD15(\epsilon N)$	1680	+0.31	+0.30	+0.29(4)

the clockwise path of the elastic amplitude on its Argand diagram (see Fig. 1). We find this state to be *much less elastic* than CMB or KH; our value for the πN branching fraction is only (9±2)%, compared with (35±6)% and (25±3)% for KH and CMB, respectively. We find a large negative $\pi\Delta$ coupling, in reasonable agreement with IC and in fair agreement with Saclay and LBL-SLAC (see Table VI). We find a small negative coupling to $(\rho_3 N)_S$, in fair agreement with Saclay, and we find a moderate positive coupling to $(\rho_1 N)_S$. The sign of our $(\rho_1 N)_S$ coupling agrees with Saclay, LBL-SLAC, and IC but the analyses disagree regarding the magnitude of the coupling. In the present work, the dominant decay mode of this state is $\pi\Delta$, with a branching fraction of (62±6)%.

$D_{33}(1700)$. We find the lowest D_{33} resonance at 1762±44 MeV, which is consistent with CMB and KH. The width is not well determined by the present work. This state is quite inelastic; the present work determines the πN branching fraction to be (14±6)%, which is consistent with CMB and KH. We find a large positive $(\pi\Delta)_S$ coupling, in good agreement with Saclay and in fair agreement with LBL-SLAC and IC (see Table VI). We find a small positive coupling to $(\pi\Delta)_D$, in good agreement with Saclay, LBL-SLAC, and IC. The various analyses do not agree very well for the ρN couplings. In the present work, the dominant decay mode of this state is $(\pi\Delta)_S$, with a branching fraction of (74±7)%.

$S_{11}(1650)$. We find the second S_{11} resonance at 1659±9 MeV with a width of 173±12 MeV. These values are consistent with CMB and KH. It has a small positive $\pi\Delta$ coupling; our value is consistent with LBL-SLAC but somewhat smaller than that of Saclay. We also find a positive coupling to $(\rho_3 N)_D$, which again is smaller than the Saclay value. We find a negligible coupling to $(\rho_1 N)_S$, whereas the LBL-SLAC and Saclay values are positive and negative, respectively. We find this state to be significantly more elastic than either KH or CMB. The present work suggests that *only* $P_{33}(1232)$ *is more elastic than this state.*

$D_{13}(1700)$. We find the second D_{13} resonance at 1737±44 MeV, which is consistent with CMB and KH. This state was not seen in the recent analysis of Arndt *et al.* [11]. In agreement with predictions of quark-model calculations (see Sec. V), all analyses find this state to be highly inelastic; in the present work, it almost completely decouples from πN and its width and couplings are essentially undetermined. The only parameter we determine for this state, other than its mass, is its $(\pi\Delta)_D$ branching fraction, which we find to be (80±19)%, making this the dominant decay mode for this state. The various analyses do not agree very well for the couplings of this state.

$D_{15}(1675)$. We find the lowest D_{15} resonance at 1676±2 MeV, which is consistent with CMB and KH. The width is 159±7 MeV, which again is consistent with CMB but somewhat larger than KH. This state decays almost 100% of the time either to πN or to $(\pi\Delta)_D$, with each mode almost equally probable. Our value for the large negative $(\pi\Delta)_D$ coupling agrees well with those of Saclay and LBL-SLAC. The resonance parameters for this state agree well among the various analyses.

B. Positive-parity states

In the following paragraphs, we discuss known members of the $N=2$ band of resonances. The $N=2$ resonances belong to five SU(6) supermultiplets: $(56,0_2^+)$, $(70,0_2^+)$, $(56,2_2^+)$, $(70,2_2^+)$, and $(20,1_2^+)$. Like the $D_{13}(1700)$ in the $N=1$ band, several states in the $N=2$ band decouple from the πN channel. In particular, states described by the dominant representation $(20,1_2^+)$ require a two-quark excitation and decouple from the channels considered in this work.

$P_{11}(1440)$. The Roper resonance is the lowest excited state with the quantum numbers of the nucleon. It is typically classified as mainly a member of the $(56,0_2^+)$ supermultiplet; i.e., it is essentially a radial excitation of the nucleon. We find this state at 1462±10 MeV, which is consistent with CMB but slightly higher than KH. The width is 391±34 MeV, which again is consistent with CMB but is significantly larger than KH. The present work determines the πN branching fraction to be (69±3)%, in good agreement with CMB, although our value is somewhat larger than that of KH. We find a large positive $(\pi\Delta)_P$ coupling, in good agreement with Saclay and LBL-SLAC. The ρN couplings for this state

as determined by Saclay and LBL-SLAC are inconsistent, while the present work finds them to be negligible. The ϵN coupling is probably large; however, the sign of this coupling as determined by the present work disagrees with both Saclay and LBL-SLAC.

$P_{33}(1600)$. The other member of the $(56,0_2^+)$ supermultiplet should be essentially a radial excitation of $P_{33}(1232)$. We find this state at 1706±10 MeV, which is *significantly higher* than either the KH value of 1522±13 MeV or the CMB value of 1600±50 MeV. (As we discuss in Sec. V, a higher mass agrees much better with quark-model calculations.) The width is 430±73 MeV, which is consistent with CMB but is significantly larger than KH. This state is fairly inelastic; the present work determines the πN branching fraction to be (12±2)%. We find a large positive $(\pi\Delta)_P$ coupling, in good agreement with Saclay, LBL-SLAC, and IC. We also find a moderate positive πN^* coupling, in reasonable agreement with IC. In the present work, the dominant decay mode of this state is $(\pi\Delta)_P$, with a branching fraction of (67±5)%.

$P_{11}(1710)$. We find the first P_{11} resonance above the Roper at 1717±28 MeV, which is consistent with CMB and KH. This state is typically classified as mainly a member of the $(70,0_2^+)$ supermultiplet. The width is not well determined by the present work. This state is quite inelastic; the present work determines the πN branching fraction to be (9±4)%, which is consistent with KH but somewhat smaller than CMB (see Table IV). We find a moderate negative $(\pi\Delta)_P$ coupling, in agreement with Saclay; the sign of this coupling differs from that of LBL-SLAC. The ρN couplings for this state as determined by Saclay and LBL-SLAC are inconsistent, while the present work finds them to be negligible. The present work also finds a negligible ϵN coupling, in disagreement with both Saclay and LBL-SLAC, which find a large negative coupling. This state is known to have a moderate coupling to $K\Lambda$, which is apparently responsible for the small cusp evident in the elastic amplitude (see the Argand diagram in Fig. 1). Recently, Cutkosky and Wang [22] carried out fits to the P_{11} data that gave similar results as CMB for this state. They used the inelastic amplitudes [5] from the Berkeley-Stanford collaboration and, as they note, "the inelastic data contribute strongly to the evidence for this resonance." We believe the results of Cutkosky and Wang must be regarded with some caution because the $\pi\Delta$ and $\rho_1 N$ couplings to $P_{11}(1710)$ found by LBL-SLAC are inconsistent with those of Saclay and the present work. The *signs* of these LBL-SLAC couplings also disagree with the quark-model predictions of Koniuk and Isgur (see Sec. V) [23]. In a recent analysis, Arndt *et al.* [11] find little evidence for this resonance and remark that, if it exists, it must be much broader than claimed by CMB and KH.

$P_{13}(1720)$. We find the first P_{13} resonance at 1717±31 MeV, which is consistent with CMB and KH. This state is typically classified as mainly a member of the $(56,2_2^+)$ supermultiplet. The width is poorly determined by the present work. This state is quite inelastic; the present work determines the πN branching fraction to be (13±5)%, which is in good agreement with KH and CMB (see Table IV). Unlike the $I=\frac{1}{2}$ states already discussed, at energies below the first resonance, the P_{13} wave is *repulsive,* as indicated by the clockwise path of the elastic amplitude on its Argand diagram (see Fig. 1). Although Saclay finds moderate negative $(\pi\Delta)_P$ and ϵN couplings for this state, neither LBL-SLAC nor the present work finds any significant couplings to those channels. The ρN couplings for this state as determined by Saclay and LBL-SLAC are inconsistent, although the present work finds a large positive $(\rho_1 N)_P$ coupling, in agreement with LBL-SLAC. In the present work, the dominant decay mode of this state is $\rho_1 N$, with a branching fraction of (87±5)%.

$F_{15}(1680)$. We find the first F_{15} resonance at 1684±4 MeV, which is in good agreement with CMB and KH. This state is mainly a member of the $(56,2_2^+)$ supermultiplet. The width is 139±8 MeV, which is slightly larger than the nominal values of CMB and KH although the values are consistent within uncertainties. This state is quite elastic; the present work determines the πN branching fraction to be (70±3)%, which again is consistent with but slightly larger than the nominal values of KH and CMB. The present work agrees remarkably well with Saclay and LBL-SLAC for the inelastic couplings of this state. It has a large negative $(\pi\Delta)_P$ coupling and a large positive ϵN coupling. It also has a moderate negative $(\rho_3 N)_P$ coupling, a small negative $(\rho_3 N)_F$ coupling, and a small positive $(\pi\Delta)_F$ coupling. The resonance parameters for this state are determined well and consistently by all of the major analyses.

$P_{31}(1910)$. We find a P_{31} resonance at 1882±10 MeV with a width of 239±25 MeV, in good agreement with CMB and KH. Two P_{31} states are expected within the $N=2$ band as mixed members of the $(56,2_2^+)$ and $(70,0_2^+)$ supermultiplets. This state is moderately elastic; the present work determines the πN branching fraction to be (23±8)%, in agreement with CMB and KH. We find a large negative coupling to πN^*, a channel not included in the Berkeley-Stanford analysis [5], which found no significant $\pi\pi N$ decays for this resonance. In the present work, the dominant decay mode of this state is πN^*, with a branching fraction of (67±10)%.

$F_{35}(1905)$. We find an F_{35} resonance at 1881±18 MeV with a width of 327±51 MeV, in good agreement with CMB and KH. Two F_{35} states are expected within the $N=2$ band as mixed members of the $(56,2_2^+)$ and $(70,2_2^+)$ supermultiplets [24]. The observed state is quite inelastic; the present work determines its πN branching fraction to be (12±3)%, in agreement with CMB and KH. We find a large positive $(\rho_3 N)_P$ coupling for this state, in good agreement with LBL-SLAC. In the present work, the dominant decay mode is $(\rho_3 N)_P$, with a branching fraction of (86±3)%.

$F_{37}(1950)$. We find the first F_{37} resonance at 1945±2 MeV, which is in good agreement with CMB but slightly higher than KH. This state is unique within the $N=2$ band and must be mainly a member of the $(56,2_2^+)$ supermultiplet. The width is 300±7 MeV, which is in good agreement with CMB but about 35% larger than the value of KH. The present work determines the πN branching fraction to be (38±1)%, in good agreement

with both CMB and KH. We find a large positive $(\pi\Delta)_F$ coupling, in good agreement with LBL-SLAC, which is the only other major work to analyze inelastic couplings in this mass region. In disagreement, however, we find no significant ρN couplings, while LBL-SLAC finds a moderate positive $(\rho_3 N)_F$ coupling. This state has a large branching fraction [(43±3)% in the present work] to channels other than πN or $\pi\pi N$.

C. New or unestablished states

We find a new P_{31} resonance at 1744±36 MeV with a width of 299±118 MeV. This state is highly inelastic; its πN branching fraction is (8±3)%. As already noted, two P_{31} states are expected within the $N=2$ band as mixed members of the $(56,2_2^+)$ and $(70,0_2^+)$ supermultiplets. The present work suggests a small positive coupling to πN^*.

We find a new F_{35} resonance at 1752±32 MeV with a width of 251±93 MeV. This state strongly decouples from the πN channel so, not surprisingly, a similar state was *not* found by CMB or KH. The present work suggests that this state has small positive couplings to $(\pi\Delta)_P$ and $(\pi\Delta)_F$ and a small negative coupling to $(\rho_3 N)_P$. As already noted, two F_{35} states are expected within the $N=2$ band as mixed members of the $(56,2_2^+)$ and $(70,2_2^+)$ supermultiplets. The more elastic F_{35} resonance is the established $F_{35}(1905)$, which we have discussed already.

We find a third D_{13} resonance at 1804±55 MeV with a width of 447±185 MeV. This state is moderately elastic; its πN branching fraction is (23±3)%. Although low in mass, this state is a candidate member of the $(56,1_3^-)$ supermultiplet [25]. A somewhat similar candidate was found by CMB at 1880±100 MeV with a width of 180±60 MeV [see $D_{13}(2090)$ in Table IV]. Also, the recent solutions KV90 and CV90 of Arndt *et al.* [11] were found to have D_{13} poles at $1900-i224$ MeV and $1926-i239$ MeV, respectively. The present work suggests a moderate negative coupling to $(\rho_3 N)_S$ and moderate positive couplings to $(\pi\Delta)_D$ and ϵN.

We find a second P_{13} resonance at 1879±17 MeV with a width of 498±78 MeV. This state is moderately elastic; the present work determines its πN branching fraction to be (26±6)% and, therefore, this state is more elastic than the lowest P_{13} resonance. This state is a candidate member of the $(70,0_2^+)$ supermultiplet. In view of its elasticity, it is rather surprising that similar candidates were not found by CMB or KH. Interestingly, the recent solutions KV90 and CV90 of Arndt *et al.* [11] were found to have P_{13} poles at $1863-i154$ MeV and $1834-i148$ MeV, respectively. The present work suggests a large negative coupling to $\rho_1 N$.

We find a third P_{11} resonance at 1885±30 MeV with a width of 113±44 MeV. This state is quite inelastic; the present work determines its πN branching fraction to be (15±6)%. This state is a candidate member of the $(70,2_2^+)$ supermultiplet. Similar candidates were found by CMB and KH [see $P_{11}(2100)$ in Table IV]. Also, the recent solution KV90 of Arndt *et al.* [11] was found to have a P_{11} pole at $1836-i93$ MeV. Not surprisingly, most of its inelastic couplings are undetermined; however, the present work suggests a moderate negative $\pi\Delta$ coupling.

We find a second F_{15} resonance at 1903±87 MeV. Its width is not well determined by the present work. This state is quite inelastic; its πN branching fraction is (8±5)%. This state is a candidate member of the $(70,2_2^+)$ supermultiplet; a somewhat similar candidate was found by KH at 1882±10 MeV [see $F_{15}(2000)$ in Table IV]. The present work suggests a moderate negative coupling to $(\rho_3 N)_P$ and small positive couplings to $(\pi\Delta)_D$ and $(\rho_3 N)_F$. In the present work, its dominant decay mode is $(\rho_3 N)_P$, with a branching fraction of (60±23)%.

We find a second S_{31} resonance at 1920±24 MeV with a width of 263±39 MeV. CMB and KH find a state at about the same mass but with a somewhat narrower width and with a smaller elasticity [see $S_{31}(1900)$ in Table IV]. The state found in the present work is quite elastic; its πN branching fraction is (41±4)%. [Note that both KH and CMB predict little inelasticity in the S_{31} wave near 1.9 GeV (see Fig. 2).] The state is a candidate member of the $(56,1_3^-)$ supermultiplet. The present work suggests a large negative coupling to $\rho_3 N$ and a moderate positive coupling to $\pi\Delta$.

We find a third S_{11} resonance at 1928±59 MeV with a width of 414±157 MeV. KH finds a state having about the same elasticity, but with a narrower width, at 1880±20 MeV. The present work suggests a moderate positive coupling to $\rho_1 N$.

We find the lowest D_{35} resonance at 1956±22 MeV with a width of 526±142 MeV. In the present work, this state is rather inelastic; its πN branching fraction is (18±2)%. Our values for the mass, width, and elasticity are in good agreement with those of CMB; KH finds this state at a slightly lower mass, with a narrower width, and a smaller elasticity [see $D_{35}(1930)$ in Table IV]. This state is a candidate member of the $(56,1_3^-)$ supermultiplet. It has no known significant $\pi\pi N$ decay modes.

We find a third P_{33} resonance at 2014±16 MeV with a width of 152±55 MeV. This state strongly decouples from the πN channel. Somewhat similar inelastic states are found by CMB and KH [see $P_{33}(1920)$ in Table V]. Only weak evidence for such a resonance was found in the recent analysis of Arndt *et al.* [11]. The present work suggests a small negative coupling to $(\pi\Delta)_P$. In the present work, this channel is the dominant decay mode with a branching fraction of (83±26)%.

We find a second D_{33} resonance at 2057±110 MeV with a width of 460±316 MeV. In general, its couplings are not well determined although the present work suggests moderate to strong positive couplings to $(\pi\Delta)_D$ and $(\rho_3 N)_S$.

We find the lowest F_{17} resonance at 2086±28 MeV, which is consistent with KH but somewhat higher than CMB. The width is 535±117 MeV, which is larger than the nominal values of CMB and KH although the values are consistent within their uncertainties. This state is

very inelastic; the present work determines its πN branching fraction to be (6±2)%, in good agreement with CMB and KH. This state is unique within the $N=2$ band and must be mainly a member of the $(70,2_2^+)$ supermultiplet. It has no known significant $\pi\pi N$ decay modes. Only weak evidence for this resonance was found in the recent analysis of Arndt *et al.* [11].

We find the lowest G_{17} resonance at 2127±9 MeV with a width of 547±48 MeV. In the present work, this state is moderately elastic; its πN branching fraction is (22±1)%. This state can be identified with $G_{17}(2190)$, a candidate member of the $(70,3_3^-)$ supermultiplet. Our values for the mass, width, and elasticity are reasonably consistent with those of CMB and KH. The present work suggests a moderate negative coupling to $(\rho_3 N)_D$.

For completeness, we mention that the present work also found a high-mass D_{35} resonance at 2171±18 MeV with a width of 264±51 MeV, which is 200–300 MeV below the second D_{35} states found by CMB and KH. It was not possible to extract inelastic couplings for this state.

D. Ratings of resonances

In this section we have discussed the resonance parameters determined by the present work and have made comparisons with prior analyses of πN elastic scattering [8,9,11] and inelastic scattering [2,3,21]. Here we evaluate the strength of evidence for each resonance using as a basis for comparison how well the total width of the resonance is determined. Table IX displays a status rating based on the estimated percentage uncertainty in the width of each resonance. Each resonance is labeled by its nominal mass taken from Ref. [10] and as identified in Tables IV and V. Here $P_{13}(1880)$, $P_{31}(1750)$, and $F_{35}(1750)$ refer to new resonances for which the present work gives some indication. If the uncertainty in the width was less than or equal to 10%, greater than 10% but less than or equal 18%, greater than 18% but less than or equal to 35%, or greater than 35%, the resonance was given a rating of four stars, three stars, two stars, or one star, respectively. Also given is an overall rating obtained by averaging results for the KSU, KH, and CMB analyses; if a resonance was not seen in one or more of the analyses, its overall rating was decreased by one star. For a four-star resonance in this system, one can expect very good agreement among different analyses for the determined values of almost all resonance parameters; for a three-star resonance, one may expect good agreement for most but not all parameters; for a two-star resonance, there is fair evidence that the resonance exists but its parameters are not likely to be determined either

TABLE IX. Status of each resonance as determined by the present work (KSU), the CMB analysis [8], and the KH analysis [9]. See the text for a description of the rating system. Also listed is the status given by the PDG [10]. Each resonance is denoted by its nominal mass value taken from the PDG [10].

Resonance	KSU	KH	CMB	Overall	PDG
$S_{11}(1535)$	***	***	**	**	****
$S_{11}(1650)$	****	***	**	***	****
$S_{11}(2090)$	*	**	**	**	*
$D_{13}(1520)$	****	****	***	****	****
$D_{13}(1700)$	*	**	*	*	***
$D_{13}(2080)$	*	***	**	**	**
$D_{15}(1675)$	****	***	***	****	****
$G_{17}(2190)$	****	****	**	***	****
$P_{11}(1440)$	****	****	**	***	****
$P_{11}(1710)$	*	***	**	**	***
$P_{11}(2100)$	*	***	*	**	*
$P_{13}(1720)$	*	***	*	*	****
$P_{13}(1880)$	***			**	
$F_{15}(1680)$	****	****	****	****	****
$F_{15}(2000)$	*	**		*	**
$F_{17}(1990)$	**	**	**	**	**
$S_{31}(1620)$	**	***	***	***	****
$S_{31}(1900)$	***	**	**	**	***
$D_{33}(1700)$	*	**	**	**	****
$D_{33}(1940)$	*		*	*	*
$D_{35}(1930)$	**	**	**	**	***
$D_{35}(2350)$	**	**	*	**	*
$P_{31}(1750)$	*			*	
$P_{31}(1910)$	****	***	**	***	****
$P_{33}(1232)$	****	****	****	****	****
$P_{33}(1600)$	***	***	**	**	**
$P_{33}(1920)$	*	*	**	**	***
$F_{35}(1750)$	*			*	
$F_{35}(1905)$	***	****	**	***	****
$F_{37}(1950)$	****	****	***	****	****

well or consistently among various analyses; finally, for a one-star resonance, there is only some evidence that it exists. In most cases, the overall ratings agree within one star of those of the Particle Data Group [10] (PDG), which have a somewhat different interpretation. Of the "established" resonances, we find a disagreement of two or more stars for $S_{11}(1535)$, $D_{13}(1700)$, $P_{13}(1720)$, and $D_{33}(1700)$; resonance parameters for these states are probably not as well determined as one might infer from their ratings by the PDG [10].

V. COMPARISONS WITH QUARK-MODEL PREDICTIONS

In the preceding section, several of the states suggested by the present work have been identified by their main component within a flavor-spin SU(6) basis. Here we present comparisons with the QCD-improved quark shell model, which is perhaps the only model that describes the baryons adequately [25]. This model uses harmonic-oscillator wave functions as a basis and includes perturbation terms suggested by one-gluon exchange. In some cases, the composition of observed states can be inferred by comparing with the predicted mass spectrum; however, for other cases where several states are predicted in the same mass range for a given partial wave, it is necessary to compare observed couplings with predicted decay amplitudes before compositions can be inferred. Although others have calculated both strong and electromagnetic decay amplitudes for the nonstrange baryons, we limit our comparisons to those of Koniuk and Isgur [23] and Forsyth and Cutkosky [25,26]. The calculations of the masses for the Koniuk-Isgur analysis are based on the work of Isgur and Karl as detailed in Ref. [27]; those for the Forsyth-Cutkosky analysis are detailed in Refs. [25] and [26]. While these calculations are similar in several aspects, configuration mixing between the $N=1$ and $N=3$ bands was considered only in the Forsyth-Cutkosky analysis. The Koniuk-Isgur analysis, however, provides important information on the *signs* of couplings to various partial-wave channels whereas the Forsyth-Cutkosky analysis provides information only on two-body and quasi-two-body partial widths.

Table X compares the theoretical decay amplitudes of Koniuk and Isgur [23] with the experimental values of the present analysis. The decay amplitudes are defined as in Ref. [23] as the square root of the partial width for a particular decay channel multiplied by the relative sign of the coupling. Note that all of the theoretical $\pi\Delta$ and ρN couplings in Table X were obtained by multiplying values from Ref. [23] by -1 to take into account an arbitrary overall sign difference between the theoretical and experimental couplings. When the meson and baryon for a decay channel have two possible values of relative orbital angular momentum, a prime is used to denote the channel having the higher angular momentum.

The resonant $\pi N \to \pi\Delta$ and $\pi N \to \rho N$ amplitudes that were determined well by the present work and that have values consistent with those determined by prior analyses (Saclay, LBL-SLAC, and IC) are marked in Tables VI and VII by an asterisk. For all of these cases, the *signs* of the couplings agree with those predicted by the quark-model calculations of Koniuk and Isgur [23]. For most of these cases, the *magnitudes* of the couplings also agree reasonably with the quark-model calculations. Notable exceptions, however, are for the $P_{11}(1440)$ and the $P_{33}(1600)$, where the theoretical $\pi\Delta$ couplings are two to four times smaller than the data. The theoretical πN coupling to $P_{11}(1440)$ is also more than two times smaller than the value determined by the present work. These inconsistencies may suggest some problem concerning the assumed wave functions of these two states, which are both mainly described by the $(56,0_2^+)$ supermultiplet. We note that our masses of 1706 ± 10 MeV for the $P_{33}(1600)$ and 1672 ± 7 MeV for the $S_{31}(1620)$ are in much better agreement with the theoretical values than are those found by CMB and KH. Also the elasticity we find for the $S_{31}(1620)$ agrees well with the quark-model prediction even though we find this state to be significantly less elastic than either CMB or KH.

Here we discuss cases where there are disagreements among the inelastic analyses (KSU, IC, LBL-SLAC, and Saclay). For the $D_{13}(1700)$, the quark-model calculations predict a large negative coupling to $(\pi\Delta)_D$, which is in agreement only with the Saclay analysis. For the $P_{11}(1710)$, the quark-model calculations predict a large negative $\pi\Delta$ coupling, which agrees in sign with results of the Saclay and present analyses, but disagrees with the LBL-SLAC analysis. The quark-model calculations predict a rather large negative $\rho_1 N$ coupling to $S_{11}(1650)$, in clear disagreement with Saclay, which finds a moderate positive coupling, although LBL-SLAC and the present work find a small to moderate negative coupling. Saclay also finds a large negative $\rho_1 N$ coupling to $P_{13}(1720)$, while both the LBL-SLAC and present analyses find large positive couplings. The quark-model calculations predict a large positive coupling, in good agreement with LBL-SLAC and the present work but in disagreement with Saclay. For the $D_{33}(1700)$, the quark-model calculations predict a large positive coupling to $(\rho_3 N)_S$, which agrees in sign with the results of Saclay and the present work, but disagrees completely with the large negative coupling of LBL-SLAC. Finally, LBL-SLAC finds a large positive $(\rho_3 N)_P$ coupling to $F_{37}(1950)$, while a large negative coupling is predicted.

One case of particular interest concerns the F_{35} wave, for which two resonances are expected in the energy range of this work. Prior elastic partial-wave analyses have suggested only a single, rather inelastic resonance near 1900 MeV, the $F_{35}(1905)$. Prior inelastic analyses have suggested that this state has a large $(\rho_3 N)_P$ decay and that the coupling to $(\pi\Delta)_F$ is larger than the coupling to $(\pi\Delta)_P$. The $\pi\Delta$ couplings were interpreted as evidence that the $(56,2_2^+)$ and $(70,2_2^+)$ configurations must be strongly mixed. The quark-model calculations of Koniuk and Isgur [23] and of Forsyth and Cutkosky [25,26] indicate that the higher-mass state should decouple from the πN channel and that the lower-mass state, identified with the observed $F_{35}(1905)$, should have mainly the $(56,2_2^+)$ configuration. The present work suggests

TABLE X. Comparison of "decay amplitudes" with the quark-model calculations of Koniuk and Isguar [23]. All masses are in MeV. See the text for a description of the notation.

Resonance	Mass	πN	$\pi\Delta$	$\pi\Delta'$	$\rho_1 N$	$\rho_3 N$	$\rho_3 N'$
$S_{11}(1535)$	1490	5.3	+1.7		−6.1	+1.6	
	1534(7)	8.8(10)	+0(1)		−1.7(5)	−1.3(6)	
$S_{11}(1650)$	1655	8.7	+8.2		−9.7	+2.7	
	1659(9)	12.4(6)	+1.7(6)		−0(1)	+2.2(9)	
$D_{13}(1520)$	1535	9.2	−6.7	−2.5	+0.7	−5.0	−1.1
	1524(4)	8.5(4)	−2.6(7)	−4.3(6)		−5.1(5)	
$D_{13}(1700)$	1745	3.6	−16	+7.7	−0.1	−4.3	−2.7
	1737(44)	2(2)	−3(4)	−14(6)		−6(6)	
$D_{15}(1675)$	1670	5.5	+9.3		−1.1	−2.0	0
	1676(2)	8.6(2)	+9.2(3)		+0.8(4)	−0.5(5)	
$P_{11}(1440)$	1405	6.8	+2.4		+0.3	+0.1	
	1462(10)	16.4(8)	+9.4(8)				
$P_{11}(1710)$	1705	6.7	−3.6		+5.5	+2.5	
	1717(28)	7(2)	−15(4)		+4(4)		
P_{11}	1890	4.4	−3.4		+4.6	−1.1	
	1885(30)	4(1)	−5(2)		+6(8)		
P_{11}	2055	1.2	−1.8		+1.2	−0.3	
	Not seen						
$P_{13}(1720)$	1710	6.5	−1.9	+1.0	+11.7	−2.6	−3.5
	1717(31)	7(1)			+18(5)		
P_{13}	1870	3.2	+4.1	+1.5	−0.4	−1.3	−0.5
	1879(17)	11(2)			−15(3)		
P_{13}	1955	1.1	+9.4	+0.7	+3.9	−6.3	−3.3
	Not seen						
P_{13}	1980	1.1	+3.4	−9.2	+7.5	−2.9	−2.3
	Not seen						
P_{13}	2060	0.5	−3.4	−4.5	−0.2	+3.3	+1.9
	Not seen						
$F_{15}(1680)$	1715	7.1	−2.0	+0.7	+1.6	−4.0	−1.3
	1684(4)	9.8(3)	−3.7(6)	+1.0(4)		−2.8(8)	−1.8(4)
F_{15}	1955	0.4	−4.7	+6.5	+1.6	+8.0	+0.7
	Not seen						
$F_{15}(2000)$	2025	1.3	+7.0	+4.3	−1.7	−6.6	−4.4
	1903(87)	6(3)	+8(6)	+2(8)		−17(6)	+9(6)
$F_{17}(1990)$	1955	3.1	+6.0		−0.8	+4.2	0
	2086(28)	6(2)					
$S_{31}(1620)$	1685	3.3	−8.0		+7.8	−1.7	
	1672(7)	3.8(8)	−10(1)		+6.1(9)	−2.5(8)	
$D_{33}(1700)$	1685	4.9	+10.3	+6.3	+4.2	+16.5	+0.9
	1762(44)	9(2)	+21(5)	+5(2)		+7(2)	

TABLE X. (*Continued*).

Resonance	Mass	πN	$\pi\Delta$	$\pi\Delta'$	$\rho_1 N$	$\rho_3 N$	$\rho_3 N'$
P_{31}	1875 1744(36)	2.7 5(1)	−7.6		+2.2	−7.6	
$P_{31}(1910)$	1925 1882(10)	5.3 7(1)	+5.9		−3.7	−4.9	
$P_{33}(1232)$	1240 1231(1)	11 10.8(2)					
$P_{33}(1600)$	1780 1706(10)	5.4 7.3(6)	+8.6 +17(2)	+0.1	−1.3	−5.5	−0.3
$P_{33}(1920)$	1925 2014(16)	5.2 2(1)	−3.2 −11(2)	−1.4	−8.1	+6.2	+5.5
P_{33}	1975 Not seen	0.1	−0.5	+7.7	−5.5	+1.8	−1.3
F_{35}	1940 1752(32)	4.0 2(1)	+3.2 +8(4)	+5.5 +11(3)	−0.05	−2.1 −7(2)	−6.4
$F_{35}(1905)$	1975 1881(18)	1.0 6(1)	−6.2 −2(3)	+1.4 +1(2)	+7.2	+17.8 +17(1)	+4.6
$F_{37}(1950)$	1915 1945(2)	7.5 10.7(1)	+5.5 +7.4(7)	0.0	−4.7	−8.2	0

a different interpretation. We were incapable of obtaining a satisfactory single-resonance fit to both the elastic and inelastic amplitudes; thus, we attempted to find a satisfactory two-resonance fit. An exhaustive number of initial parameter values were tried using various combinations of coupling signs for all of the inelastic channels. A successful two-resonance fit was finally obtained with the resonance parameters summarized in Table III. We found the more elastic resonance at 1881±18 MeV with its total width and elasticity in reasonable agreement with values for the $F_{35}(1905)$ found in the elastic analyses (see Table V). If this state were identified with the lower-mass quark-model state, which is mainly $(56,2_2^+)$, we would expect to find the second, more inelastic resonance to have a mass greater than 1900 MeV [24]. Surprisingly, we instead found the second, more-inelastic resonance at a lower energy, specifically at 1752±32 MeV. The signs and magnitudes of the inelastic couplings for these two states suggest the identification made in Table X. Both of the observed states, so identified, are about 150 MeV lower in mass than the quark-model predictions. These discrepancies in mass and elasticity might be evidence for mixings with the $N=4$ band, which were not considered in any of the quark-model calculations.

As mentioned already, the Forsyth-Cutkosky analysis [25,26] considered mixing between the $N=1$ and $N=3$ bands; however, neither the Koniuk-Isgur analysis [23] nor the Forsyth-Cutkosky analysis considered mixing between the $N=2$ and $N=4$ bands. Table XI compares masses and partial widths calculated by Forsyth and Cutkosky (theory) with the values (data) of the present work. Only states predicted to have masses below 2200 MeV are included in the table, since we generally did not fit elastic amplitudes at higher energies. The identification of a predicted state with a particular observed state is sometimes quite speculative and occasionally relies on decay amplitudes from the Koniuk-Isgur analysis. In general, the masses of negative-parity baryons predicted with the larger basis of Forsyth and Cutkosky agree better with the values of the present work than do those predicted by Isgur and Karl [27]. The dominant decay channel(s) for a resonance are probably more evident in Table XI than in Table X. For example, the second S_{11} resonance is predicted to be very elastic, in good agreement with our large πN partial width for that state. Also the second D_{13} resonance is predicted to have a dominant $\pi\Delta$ decay mode, consistent with our $\pi\Delta$ branching fraction of about 85%. Perhaps a serious discrepancy occurs for the second S_{31} state, which is an $N=3$ state near 1900 MeV. The calculation of Forsyth and Cutkosky indicates very little elasticity in this mass region while the experimental partial-wave cross section (see Fig. 2) indicates very little inelasticity. The lowest D_{35} resonance (another $N=3$ state) is predicted to decouple from the $\pi\Delta$ and ρN channels; this prediction seems to be born out by experiment.

VI. SUMMARY AND CONCLUSIONS

This work was undertaken primarily to study nucleon resonances using the isobar-model partial-wave ampli-

TABLE XI. Comparisons of masses and partial widths (in MeV) with the quark-model calculations of Forsyth and Cutkosky [25,26]. Only states predicted to have masses below 2200 MeV are listed.

	Data		Theory			
State	Mass	πN	Mass	πN	$\pi\Delta$	ρN
S_{11}	1534(7)	77(17)	1530	32	14	4
	1659(9)	173(12)	1643	102	19	11
			1809	10	36	14
			2059	1	3	23
	2149(23)	110(60)	2151	7	4	5
D_{13}	1524(4)	73(6)	1529	66	25	3
	1737(44)	3(7)	1682	18	113	39
	1804(55)	104(40)	1809	12	8	1
			2066	24	3	11
			2194	11	15	39
D_{15}	1676(2)	74(4)	1661	66	85	1
			2168	22	14	56
G_{17}	2127(9)	123(14)	2167	66	9	79
P_{11}	1462(10)	270(25)	1383	81	15	0
	1717(28)	45(22)	1714	12	24	9
	1885(30)	17(11)	1957	6	5	1
			2075	2	0	52
P_{13}	1717(31)	50(16)	1768	33	28	23
	1879(17)	130(37)	1882	10	42	21
			1950	3	12	2
			1974	1	75	23
			2138	2	27	35
F_{15}	1684(4)	96(6)	1684	83	7	13
			1995	5	23	10
	1903(87)	39(33)	2088	0	173	18
F_{17}	2086(28)	34(18)	1990	0	71	0
S_{31}	1672(7)	14(6)	1643	26	91	17
	1920(24)	107(22)	1935	0	0	2
			2171	1	16	6
D_{33}	1762(44)	81(34)	1676	17	78	5
			1926	5	6	4
	2057(110)	81(104)	2170	17	9	19
D_{35}	1956(22)	93(24)	1931	27	3	2
P_{31}	1744(36)	24(13)	1906	7	6	11
	1882(10)	55(22)	1946	1	8	11
P_{33}	1231(1)	118(4)	1232	134	0	0
	1706(10)	53(9)	1787	48	4	1
	2014(16)	3(4)	1924	1	91	34
			2036	2	27	16
F_{35}	1752(32)	4(3)	1894	37	84	28
	1881(18)	41(13)	2082	1	8	43
F_{37}	1945(2)	114(2)	1945	93	76	16

tudes of the Virginia Tech solution [1]. In the Virginia Tech analysis, over 30% more $\pi N \to \pi\pi N$ events (241 214 events in all) were included than in the previous Berkeley-SLAC analysis [5]. The Virginia Tech analysis was the first to investigate πN partial waves with $l > 3$ and to investigate resonance couplings to the πN^* channel using both $\pi^- p$ and $p^+ p$ data. (An Imperial College group [21] had previously investigated resonance couplings to πN^* using just $\pi^+ p$ data.) The Virginia Tech analysis included data up to 1930 MeV while the Berkeley-SLAC analysis [5] included data up to 2000 MeV. Another major isobar-model analysis [4] by a group at Saclay included data up to 1760 MeV; the Imperial College analysis [21] included data only up to 1700 MeV. Therefore, of the major isobar-model analyses, only those of the Virginia Tech and Berkeley-SLAC groups investigated resonance couplings at center-of-mass energies above about 1750 MeV. Of these, the latter used a low-momentum approximation for barrier-penetration factors (as did Imperial College); this approximation is known to suppress certain partial-wave amplitudes [4]. The Saclay group used a penetration factor similar to the Blatt-Weisskopf form used by the Virginia Tech group, which does not lead to such problems. There have also been concerns [24], regarding the determination of the overall phase for the Berkeley-SLAC amplitudes at energies above 1800 MeV. In particular, the Berkeley-SLAC FF37($\pi\Delta$) amplitude requires a "background phase" of about 70°, which is difficult to understand. Because of these known deficiencies of the Berkeley-SLAC amplitudes and because of various inconsistencies between the Berkeley-SLAC amplitudes and those of the Virginia Tech and Saclay solutions, we felt it important to perform a new and independent investigation of resonance parameters based on the Virginia Tech amplitudes. A detailed comparison of the major isobar-major analyses mentioned here is discussed in Ref. [1].

In this work, various Breit-Wigner parameters have been extracted from the isobar-model amplitudes of Ref. [1] and the elastic amplitudes of Refs. [8] and [9]. The present work uses a novel unitary, multichannel, multiresonance parametrization that incorporates nonresonant background. In addition to the information obtained for established resonances, we also find some evidence for new resonances, including a P_{31} state at 1744±36 MeV, an F_{35} state at 1752±32 MeV, and a P_{13} state at 1879±17 MeV. Only weak evidence was found for the "established" D_{13}, P_{11}, and P_{13} resonances with masses near 1700 MeV. When compared with results of elastic phase-shift analyses, the masses and widths determined in the present work generally agree better with those of the Carnegie-Mellon–Berkeley (CMB) solution [8] than with those of the Karlsruhe-Helsinki (KH) solution [9]. In particular, the widths of the KH solution tend to be smaller than those found in the present work and in the CMB solution. When compared with results of previous inelastic analyses [2,3,21], there is generally good agreement for the signs and magnitudes of $\pi\Delta$ couplings but poor agreement for the smaller ρN couplings. There is especially good agreement among the various analyses [2,3,8,9] for the masses, widths, and couplings of the $D_{13}(1520)$, $D_{15}(1675)$, $F_{15}(1680)$, and $F_{37}(1950)$ resonances. When compared with quark-model calculations [23], the couplings determined in the present work agree, on the whole, surprisingly well with predicted values. Our results therefore lend credence to the single-quark transition model for baryon decays. Hopefully new experiments, such as those planned for CEBAF [28], will help confirm the existence of some of the more inelastic resonances proposed by this work.

Notes added.

(1) After we had submitted this manuscript for publication, it was suggested to us by Cutkosky [29] that perhaps a more natural description of the physics would be given by a parametrization in which the resonance factor was interior and was pre- and postmultiplied by background factors, which need not be diagonal. (His reasoning is based on the standard view that the resonances involve a short-range interaction among quarks, while the background represents long-range effects. This view is consistent with the fact that the sign of the elastic background phase at low energies is given by simple models involving u- and t-channel exchanges. In such a case, the background amplitude is given by incoming and outgoing wave functions that are matched to the interior wave functions at some small distance.) We would like to point out that, while various parametrizations for describing πN scattering abound, none are completely ideal and there is no "standard" multichannel parametrization. In our work, we purposely and necessarily kept our background parametrization as *simple* as possible. Consequently, only a single (nondiagonal) background factor was introduced, which was constructed to require the minimum number of parameters that could be deduced reasonably from the data. Cutkosky also expressed concern regarding the analyticity properties of our parametrization and the possible influence on the derived resonance parameters. While we believe that none of our approximations seriously affect the extracted resonance parameters, we concede that further study of the analytic properties of our amplitudes is warranted. Finally, we note that as with *any* such analysis, our results should be most reliable for strongly excited resonances that are reasonably well separated from other states and large background contributions.

(2) The inelastic partial-wave cross sections shown in Fig. 2 show that the results from elastic partial-wave analyses give large fluctuations at the lower energies. Cross-section measurements for the $\pi N \to \pi\pi N$ reactions can provide important constraints on the inelastic partial-wave cross sections, particularly near threshold. In 1984, one of us (D.M.M.) published a global analysis of all available low-energy data for the $\pi N \to \pi\pi N$ reactions in terms of isospin amplitudes [30]. Since then, several new measurements for the $\pi N \to \pi\pi N$ reactions were performed near threshold for the purpose of studying chiral-symmetry-breaking terms in the low-energy $\pi\pi$ and πN systems. After our manuscript was submitted for publication, a new global analysis of all available data

near threshold was published by Burkhardt and Lowe [31]. Interested readers will find references for the new measurements in their paper.

(3) After our manuscript was submitted for publication, additional evidence for our P_{13} resonance candidate at 1879±17 MeV was given by Höhler in an invited talk at Saclay [32]. A "speed plot" using the Karlsruhe solutions KH80 [9] and KA84 [16] for the P_{13} partial wave gives a peak near 1900 MeV, which had not been reported previously. Its height is compatible with the width and elasticity given by our present analysis.

ACKNOWLEDGMENTS

We thank R. A. Arndt, R. E. Cutkosky, and G. Höhler for helpful comments. This work was supported in part by the National Science Foundation under Grants No. PHY-8902479 and PHY-9106512.

[1] D. M. Manley, R. A. Arndt, Y. Goradia, and V. L. Teplitz, Phys. Rev. D **30**, 904 (1984).
[2] R. S. Longacre and J. Dolbeau, Nucl. Phys. **B122**, 493 (1977).
[3] R. S. Longacre, T. Lasinski, A. H. Rosenfeld, G. Smadja, R. J. Cashmore, and D. W. G. S. Leith, Phys. Rev. D **17**, 1795 (1978).
[4] J. Dolbeau, F. A. Triantis, M. Neveu, and F. Cadiet, Nucl. Phys. **B108**, 365 (1976).
[5] D. J. Herndon, R. Longacre, L. R. Miller, A. H. Rosenfeld, G. Smadja, P. Söding, R. J. Cashmore, and D. W. G. S. Leith, Phys. Rev. D **11**, 3183 (1975).
[6] S. Almehed and C. Lovelace, Nucl. Phys. **B40**, 157 (1972).
[7] R. Ayed, P. Bareyre, and Y. Lemoigne, contributed paper to the XVIth International Conference on High Energy Physics, Chicago-Batavia, Illinois, 1972 (unpublished).
[8] R. L. Kelly and R. E. Cutkosky, Phys. Rev. D **20**, 2782 (1979); R. E. Cutkosky, R. E. Hendrick, J. W. Alcock, Y. A. Chao, R. G. Lipes, J. C. Sandusky, and R. L. Kelly, *ibid.* **20**, 2804 (1979); R. E. Cutkosky, in *Baryon 1980,* Proceedings of the IVth International Conference on Baryon Resonances, Toronto, 1980, edited by N. Isgur (University of Toronto, Toronto, 1980), p. 19.
[9] G. Höhler, F. Kaiser, R. Koch, and E. Pietarinen, *Handbook of Pion-Nucleon Scattering* [Physics Data No. 12-1 (1979)]; G. Höhler, in *Pion-Nucleon Scattering,* edited by H. Schopper, Landolt-Börnstein, New Series, Group 1, Vol. 9, Pt. b (Springer, New York, 1983); R. Koch, in *Baryon 1980* [8], p. 3; R. Koch and E. Pietarinen, Nucl. Phys. **A336**, 331 (1980).
[10] Particle Data Group, J. J. Hernández *et al.,* Phys. Lett. B **239**, 1 (1990), p. I.1.
[11] R. A. Arndt, Z. Li, L. D. Roper, R. L. Workman, and J. M. Ford, Phys. Rev. D **43**, 2131 (1991).
[12] D. E. Novoseller, Nucl. Phys. **B176**, 153 (1980).
[13] J. M. Blatt and V. F. Weisskopf, *Theoretical Nuclear Physics* (Wiley, New York, 1952); also see Ref. [1] for explicit representations of the barrier penetration factors.
[14] R. A. Arndt (private communication).
[15] P. R. Bevington, *Data Reduction and Error Analysis for the Physical Sciences* (McGraw-Hill, New York, 1969).
[16] R. Koch, Z. Phys. C **29**, 597 (1985).
[17] G. Höhler, D. Grether, M. Hutt, and I. Sabba-Stefanescu, Karlsruhe Report No. TKP 83-24, 1983 (unpublished).
[18] R. Koch, Nucl. Phys. **A448**, 707 (1986).
[19] G. Höhler, in *Proceedings of the Twelfth International Conference on Few Body Problems,* Vancouver, British Columbia, 1989, edited by H. W. Fearing [Nucl. Phys. **A508**, 525c (1990)]; in Proceedings of the Third International Symposium on Pion-Nucleon and Nucleon-Nucleon Physics, Gatchina, USSR, 1989 (unpublished), p. 15.
[20] Particle Data Group, J. J. Hernández *et al.,* Phys. Lett. B **239**, 1 (1990), p. VIII.9.
[21] K. W. J. Barnham, S. L. Glickman, W. A. C. Mier-Jedrzejowicz, S. J. Orebi Gann, R. A. Stevens, and A. P. White, Nucl. Phys. **B168**, 243 (1980).
[22] R. E. Cutkosky and S. Wang, Phys. Rev. D **42**, 235 (1990).
[23] R. Koniuk and N. Isgur, Phys. Rev. D **21**, 1868 (1980); R. Koniuk, Nucl. Phys. **B195**, 452 (1982).
[24] D. M. Manley, Phys. Rev. Lett. **52**, 2122 (1984).
[25] C. P. Forsyth and R. E. Cutkosky, Z. Phys. C **18**, 219 (1983).
[26] C. P. Forsyth, Ph.D. dissertation, Carnegie-Mellon University, 1981.
[27] N. Isgur and G. Karl, Phys. Rev. D **18**, 4187 (1978); **19**, 2653 (1979).
[28] V. Burkert, Research Program at CEBAF (II), 161 (1987).
[29] R. E. Cutkosky (private communication).
[30] D. M. Manley, Phys. Rev. D **30**, 536 (1984).
[31] H. Burkhardt and J. Lowe, Phys. Rev. Lett. **67**, 2622 (1991).
[32] G. Höhler, in Proceedings of the Workshop on Baryon Spectroscopy and the Structure of the Nucleon, Saclay, France, 1991 (unpublished).